Revista Română de Inginerie Civilă

Indexată în bazele de date internationale (BDI)

ProQuest, INSPEC, EBSCO, GOOGLE SCHOLAR, CROSSREF, TDNET, DIMENSIONS, DRJI, JGATE, INDEX COPERNICUS, ULRICH'S și JOURNALSEEK

Volumul 13 (2022), Numărul 4

Smart parking monitoring software application

Aplicație software inteligentă de monitorizare a parcării *309-319*

Cristina Gabriela Sărăcin, Florin Daniel Streche

Nitrates removal from water using ion exchange technologies

Eliminarea nitraților din apă folosind tehnologii de schimb ionic *320-336*

Alexandru Matei, Elena Vulpaşu, Gabriel Racoviţeanu

Simplified procedure for evaluating energy performance of heat pumps. Energy and economic analysis

Procedura simplificată de evaluare a performanței energetice a pompelor de căldură. Analiza energetica si economica *337-352*

Florin Iordache, Mugurel Talpiga

Influența generatoarelelor sincrone cu magneți permanenți în industria energiei regenerabile

The influence of permanent magnet synchronous generators in the renewable energy industry *353-363*

Emilia Dobrin

Cheap building material prepared by unconventional heating of glass waste in alkaline solution

Material de construcție ieftin fabricat prin încălzirea neconvențională a deșeului de sticlă în soluție alcalină *364-374*

Lucian Păunescu, Sorin-Mircea Axinte

MATRIX ROM
OP CHIAJNA CP 2
077040 – ILFOV
Tel. 021 4113617 Fax. 021 4114280
e-mail: office@matrixrom.ro
www.matrixrom.ro

EDITORIAL BOARD

Ph.D. R.S.AJIN, *Kerala State Disaster Management Authority, India*
Ph.D.Prof.Eng. Ioan BOIAN, *Transilvania University of Brasov, Romania*
Ph.D.Prof.Eng. Ioan BORZA, *Polytechnic University of Timisoara, Romania*
Ph.D.Assoc.Prof.Eng. Vasilică CIOCAN, *Gh. Asachi Technical University of Iaşi, Romania*
Ph.D.Prof. Stefano CORGNATI, *Politecnico di Torino, Italy*
Ph.D.Assoc.Prof.Eng. Andrei DAMIAN, *Technical University of Constructions Bucharest, Romania*
Ph.D.Prof. Yves FAUTRELLE*, Grenoble Institute of Technology, France*
Ph.D.Prof.Eng. Carlos Infante FERREIRA*, Delft University of Technology, The Netherlands*
Ph.D.Prof. Manuel GAMEIRO da SILVA*, University of Coimbra, Portugal*
Ph.D.Prof.Eng. Dragoş HERA, *Technical University of Constructions Bucharest, Romania, honorary member*
Ph.D. Jaap HOGELING, *Dutch Building Services Knowledge Centre, The Netherlands*
Ph.D.Prof.Eng. Ovidiu IANCULESCU, *Romania*, *honorary member*
Ph.D.Lawyer Cristina Vasilica ICOCIU, *Polytechnic University of Bucharest, Romania*
Ph.D.Prof.Eng. Anica ILIE, *Technical University of Constructions Bucharest, Romania*
Ph.D.Prof.Eng. Gheorghe Constantin IONESCU, *Oradea University, Romania*
Ph.D.Prof.Eng. Florin IORDACHE, *Technical University of Constructions Bucharest, Romania* – ***director editorial***
Ph.D.Prof.Eng. Vlad IORDACHE, *Technical University of Constructions Bucharest, Romania*
Ph.D.Prof.Eng. Karel KABELE*, Czech Technical University, Prague, Czech Republic*
Ph.D.Prof. Birol KILKIS, *Baskent University, Ankara, Turkey*
Ph.D.habil. Assoc.Prof. Zoltan MAGYAR, *Budapest University of Technology and Economics, Hungary*
Ph.D.Assoc.Prof.Eng. Carmen MÂRZA, *Technical University of Cluj Napoca, Romania*
Ph.D.Prof.Eng. Ioan MOGA, *Technical University of Cluj Napoca, Romania*
Ph.D.Assoc.Prof.Eng. Gilles NOTTON, *Pascal Paoli University of Corsica, France*
Ph.D.Prof.Eng. Daniela PREDA, *Technical University of Constructions Bucharest, Romania*
Ph.D.Prof.Eng. Adrian RETEZAN, *Polytechnic University of Timisoara*, *Romania*
Ph.D. Boukarta SOUFIANE, *Institute of Architecture and Urban Planning, BLIDA1, Algeria*
Ph.D.Assoc.Prof.Eng. Daniel STOICA, *Technical University of Constructions Bucharest, Romania*
Ph.D.Prof. Branislav TODOROVIĆ, *Belgrad University, Serbia*
Ph.D.Prof. Marija S. TODOROVIĆ, *Academy of Engineering Sciences of Serbia*
Ph.D.Eng. Ionuţ-Ovidiu TOMA, *Gh. Asachi Technical University of Iaşi, Romania*
Ph.D.Prof.Eng. Ioan TUNS, *Transilvania University of Brasov, Romania*
Ph.D.Assoc.Prof.Eng. Constantin ŢULEANU, *Technical University of Moldova Chisinau, Republic of Moldova*
Ph.D.Assoc.Prof.Eng. Eugen VITAN, *Technical University of Cluj Napoca, Romania*

Romanian Journal of Civil Engineering is founded, published and funded by publishing house MATRIX ROM
Executive Director: mat. Iancu ILIE

Online edition ISSN 2559-7485
Print edition ISSN 2068-3987; ISSN-L 2068-3987

Smart parking monitoring software application

Aplicație software inteligentă de monitorizare a parcării

Cristina Gabriela Sărăcin[1], Florin Daniel Streche[1]

[1]Universitatea Polithnica din București, România
Splaiul Independenței Nr.313
E-mail: cristina.saracin@upb.ro, daniel.streche@yahoo.com

DOI: 10.37789/rjce.2022.13.4.1

Abstract.– *The paper presents the software application designed to monitor the car parking occupancy rate. The real situations that can be encountered in a parking lot are simulated with the help of a scale model made based on the Raspberry Pi 3 development board. This board connects the existing hardware components on the scale model, the created software applications, and the Cloud Firebase database. The services offered by Firebase use the real-time database and the authentication service. The first is used to store data received from parking sensors and the second to register and authenticate car parking users. The user interface is made within the Android Studio programming environment. The developed applications are the followings: new user account registration, user authentication, parking space reservation, parking entrance, parking space occupation and parking exit. The smart car parking collects real-time information which contributes to diminish the time spent in traffic, decreases pollution, and why not, significantly reduces of the stress of the drivers.*

Keywords: smart car parking, Cloud Firebase, Android Studio, Raspberry Pi 3 Board

1. Introduction

The study conducted by the Statista company shows that, from 2006 to 2015, the number of personal cars increased from 679 to 947 million vehicles and, the number of commercial transport vehicles increased from 247 to 335 million units [1]. In 2021 it is globally estimated a total of 1.4 billion cars, which means an increase of over 100 million compared to 2015.

The study conducted by the company Inrix shows that American drivers spend an average of 17 hours per year to find a parking space and for this they annual pay $345. Almost two-thirds of Americas drivers (61%) reported they felt stressed trying to find a parking spot, nearly half (42%) missed an appointment, one-in-three (34%) abandoned a trip due to parking problems and one-quarter (23%) experienced road rage [2].

It is also estimated that the urban population will significantly increase in the coming decades, from the current 3.9 billion (54% of the total global population) to 6.3 billion by 2050. These increases implicitly lead to a real explosion in the number of

vehicles, which dramatically amplifies the time spent in traffic and a much higher level of pollution than at present time.

All the studies presented lead to the widespread implementation of the notion of smart city. The smart city is the city concept that uses the digital, information and communications technologies for support of human lives quality in a city. For realization of concept objectives, it is necessary so the city might the high quality and safe information and communicational system [3]. The concept of smart city entails the fluidization of traffic and the emergence of smart parking. Smart Cities are a current emerging trend that aims to effectively and smartly automate the monitoring, access and usage of the infrastructure underpinning the major services offered to the citizens. Advanced wireless sensing technologies, machine learning techniques, 5G networks and big data analytics tools are among the main enablers of secure and effective management of the often-limited city resources. If its usage is properly optimized such resources can significantly assist in revolutionizing the citizens life through improved education, better and more affordable healthcare and cheaper, greener and more comfortable transport [4]. A “smart city” is not a particularly new concept. Urban planners and city governments have been implementing automated or digital solutions to provide improved services for years. A “smart city” is about more than the sum of the automation and digital endeavours [5].

A novel parking management system consists of hardware and software modules. On the hardware side, Raspberry Pi device is used along with few other parts like sensors and cameras. On the software side, python modules are implemented with efficient data-management. For example, it can be modelled different possible actions of the drivers and ensured that the proposed parking system performs perfectly. In car parking case, three core situations can be outlined. First one is when drivers park correctly, the second one has error-correction, and the third one requires error correction involving multiple cars. This system can be used in any large parking structure in the modern smart cities [6].

This paper intends to develop a smart car parking model and implement software applications to monitor it.

2. Smart parking monitoring simulation model

The hardware components used to simulate smart parking monitoring are as follows:

- development board Raspberry Pi 3 model B +;
- two Digital Sharp GP2Y0D810Z0F distance sensors;
- Raspberry Pi v2.1 video camera;
- barrier’s servomotor;
- conductive elements and breadboard.

The camera is used to signal the entry of a car into the parking area and at the same time to read the registration number. It also commands the actuator that closes or opens the barrier. The servomotor is SG90 type with supply voltage of 4.8V with rotational speed of 0.12s/60˚ and 0.11s/60 ˚ for a voltage of 6V. Also the rotation angle is 180 degrees. It was connected to terminal 2 of the Raspberry Pi development board. The

integrated network of the development board is connected to an external Wi-Fi network through which the data is transmitted to the parking database. The operating system of the development board is Rasbian. This software runs from a micro-SD card inserted in the dedicated port located on the development board. The programming of sensors and other hardware components is done based on the Python programming language. The two Digital Sharp distance sensors provide information regarding occupancy of parking space. The two distance sensors use infrared technology to detect objects. The supply voltage of this sensor module is between 2.7 and 6.2V. The detection range of an object is between 2 and 10cm. The two sensors were connected to pins 1 and 4 of the Raspberry Pi development board.

The block diagram of the proposed intelligent parking system is shown in Figure 1. It can be seen the moments when, the GSM application and the program running on the Raspberry Pi card exchange information with the Firebase database. A JSON (JavaScript Object Notation) file is required to connect the hardware and software components to the cloud database. JSON is a standard format that helps to transmit data between a server and a web application. It is also an alternative to XML [12]. The JSON file was downloaded after the Firebase cloud database was created and added to the mobile application file package and Raspberry Pi development board memory.

At the same time, it can be observed the steps the driver must go through when he enters into the parking area, as well as the way hardware components operate.

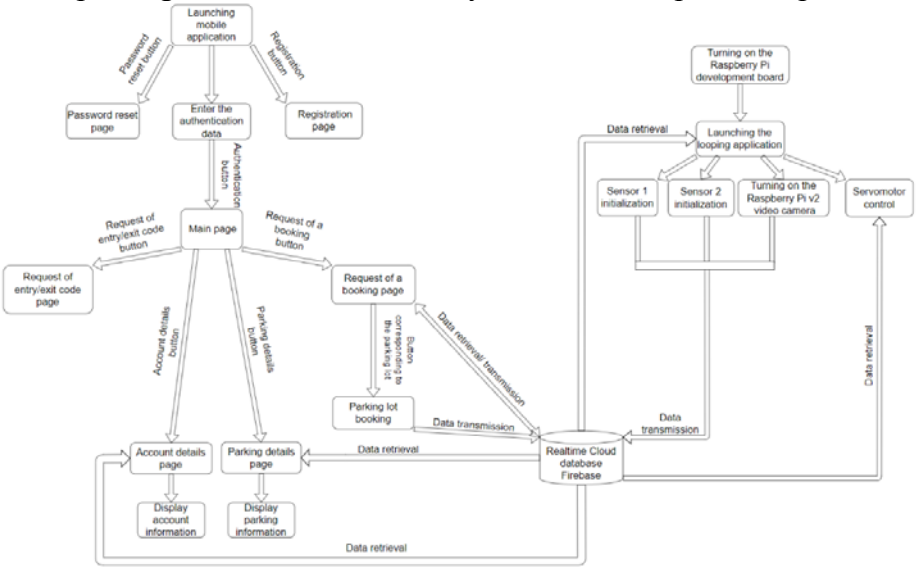

Fig. 1 Block diagram of smart parking system

As it can be seen in figure 1, the program runs on the Raspberry Pi, it takes the information from the distance sensors and the Raspberry Pi v2 camcorder and, transmits it to the database. If the parking space is not occupied, the sensor is in standby, and the program sends the "Free" information to the database. If the parking space is occupied, the sensor is activated, and the program sends the "Busy" information to the database. The camcorder transmits the image to the Raspberry Pi device, and with the help of the program, this processed info enables the scanning of the QR code displayed on the

driver's mobile phone. When the QR code is recognized in the database, the servomotor commands the lifting of the access barrier of the entry or exit smart parking. In figure 1 is also shown the bidirectional transmission between the application installed on the mobile phone and the database of the smart parking.

3. Smart car parking monitoring software application

The developed model of monitoring parking spaces consists of the following elements and subsystems:

- entrance/exit system in/from the parking lot;
- system for taking over the data from the parking places;
- GSM interface, consisting of the following pages:
    - New user registration;
    - User authentication;
    - Password reset;
    - Main program;
    - Parking details;
    - Account details;
    - Request a reservation;
    - Requests a code for entering/exiting the car parking.
- cloud database for data storage;
- payment monitoring method.

The software application is implemented in the Android Studio program and is dedicated to cell phones that use the Android operating system [7].

3.1. New user registration

The driver must register if using the car parking for the first time. He can create a new account by pressing the "REGISTER" button in the GSM application running on his phone. The registration page contains the following details:

- name and surname;
- valid e-mail address;
- password;
- phone number;
- registration number of the car.

After completing all the fields, the user is entered in the Firebase authentication service (Fig. 2.) and in the database (Fig. 3).

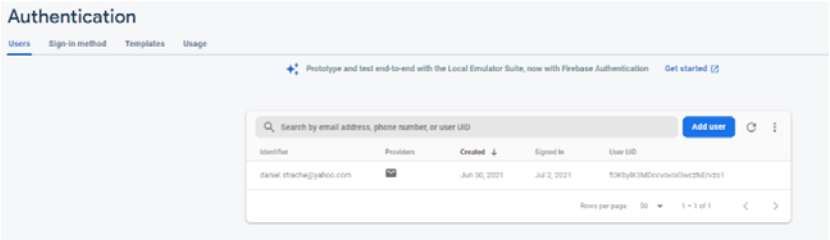

Fig. 2 Entering new user to the Firebase authentication service

At this time a verification email is sent to the driver's email address (Fig. 4). The code sequence required to register a new user is shown in Figure 3. After registration, if all data has been entered correctly, the app will go to the "Login" page. If the user did not fill in the info required for registration correctly, the error message “Registration failed” will appear. An example of an error, it is when the driver wants to register an account with an e-mail address already existing in the database.

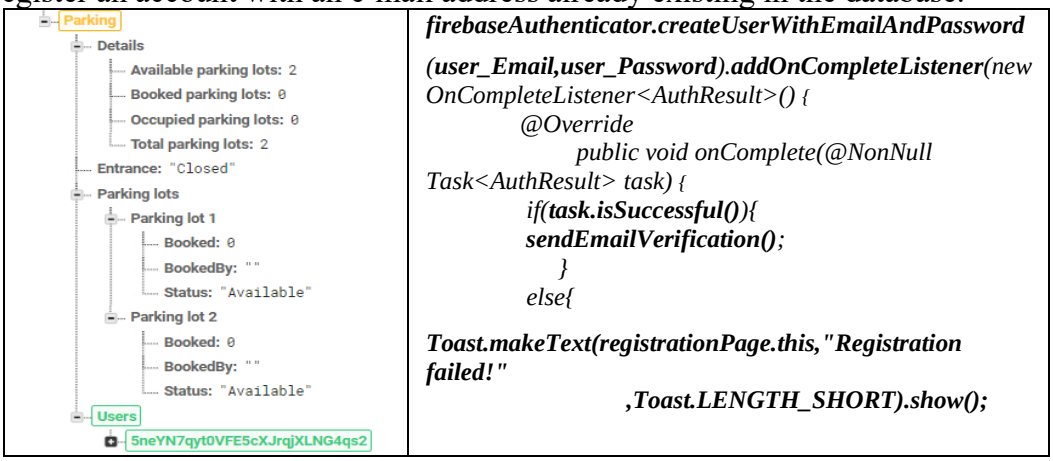

Fig. 3 Entering new user in the Firebase database

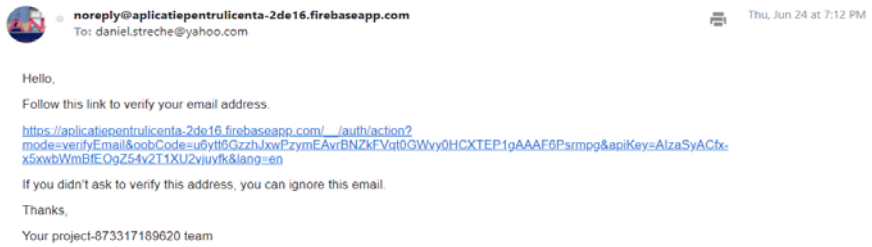

Fig. 4 Email address validation

3.2. User authentication

After entering and verifying the account, the user logs in by entering the email address and password in the corresponding fields on the Login page.

If the e-mail or password is incorrect, the error message "Login failed!" appears (Fig. 5). Figure 5 also shows the code sequence required for authentication.

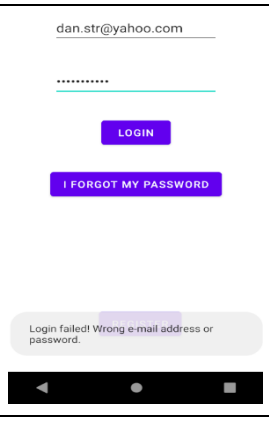


```
firebaseAuthenticator.signInWithEmailAndPassword(firstName,
userPassword).
addOnCompleteListener(new OnCompleteListener<AuthResult>() {
        @Override
        public void onComplete(@NonNull Task<AuthResult> task)
{
            if(task.isSuccessful()){
               emailVerification();
               finish();
        }
            else{
            Toast.makeText(MainActivity.this,"Login failed!
Wrong e-mail address or
password.",Toast.LENGTH_SHORT).show();
        }
```

Fig. 5 Failed authentication message

If the driver has forgotten the password, the "I FORGOT MY PASSWORD" button can be used. If the email completed by the user is correct (the one from which the account was created) then, a password reset email is sent to that account. Accessing the link (shown in fig. 6) allows to reset the password.

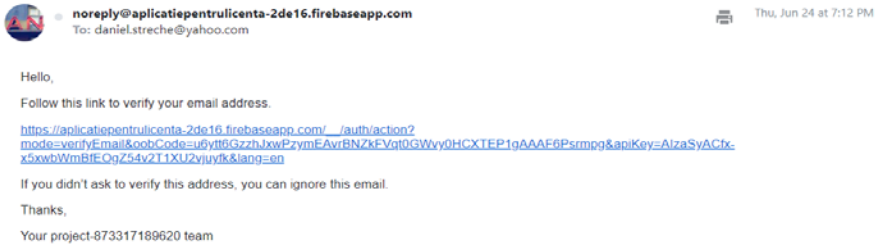

Fig. 6 Password reset email

3.3. Parking space reservation

After the user's authentication, the main page of the graphical interface opens, providing access to the page with parking details, account details, plus a new booking request.

In the parking details page, the user is provided with data on the total number of parking spaces, vacancies, occupied, reserved and the status of the barrier at the parking area entrance.

On the reservation request page, the user can make a reservation of a certain parking lot by pressing the button corresponding to the desired parking space ("PARKING LOT 1" or "PARKING LOT 2"). This page also provides information on parking spaces, namely:

- if they are free, the colour of the buttons is green;
- if they are busy, the colour of the buttons is red;
- if they are reserved, the colour of the buttons is orange;

and, also information on who reserved the parking lot by identifying the registration number (Fig. 7).

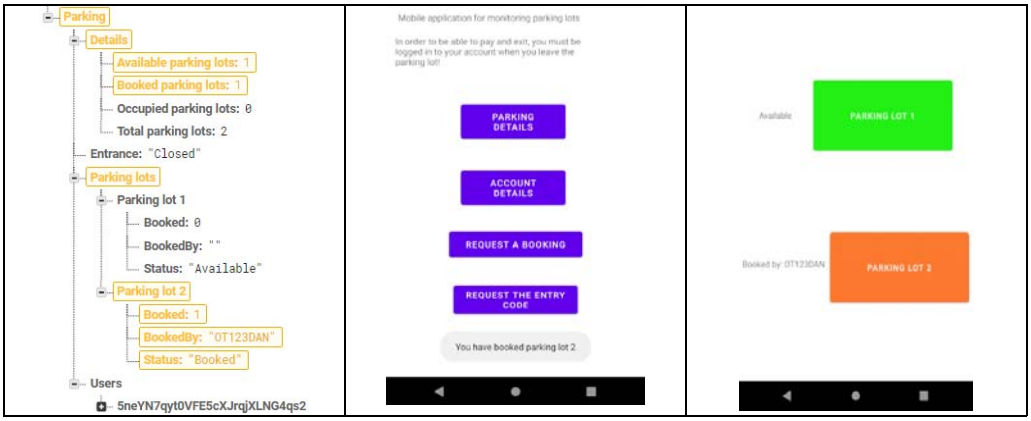

Fig. 7 Updating data in the database after booking Parking lot 2

To reserve a parking space, the button corresponding to the desired parking lot must be pressed. If the place is already reserved, an error message is displayed the following text: parking space "Occupied" or "Reserved".

3.4. Car parking entrance procedure

The car parking entrance code can only be requested if the driver has first reserved a parking space; otherwise, an error message is received. The request of the parking entry code is made by pressing the “REQUEST THE ENTRY CODE” button (Fig. 8). The parking entry request page shows a QR Code image that is required to enter the parking area. The driver positions the phone display in front of the Raspberry Pi v2 digital camera and, after scanning the QR code, the barrier rises. After a certain pre-set time, the barrier is closed, the access to the parking area being blocked.

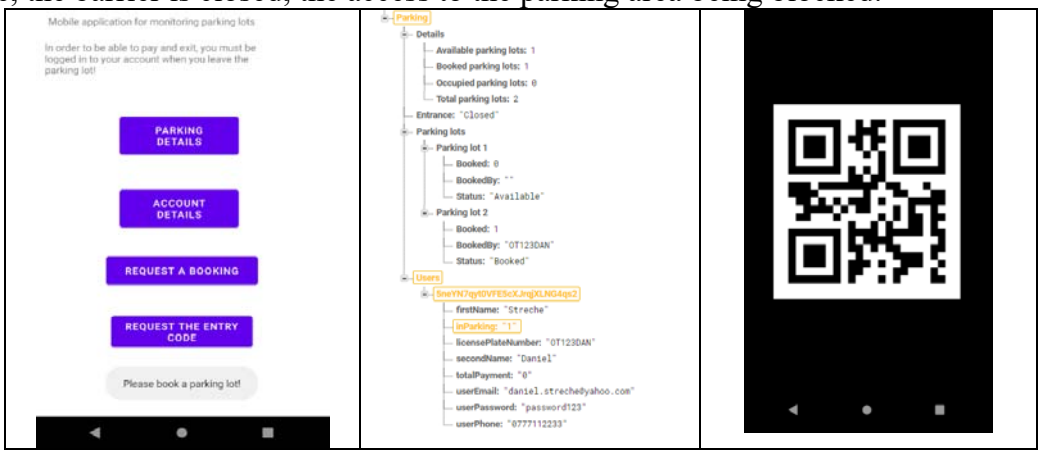

Fig. 8 Booking a parking lot and updating info in database at the request of the entry code

After booking a parking space and entering the parking area, the driver must go to the reserved parking lot to occupy it.

3.6. Occupancy of the parking space

At this moment, the distance sensors related to the respective parking space update the database with the new occupancy of the parking lot (Fig. 9).

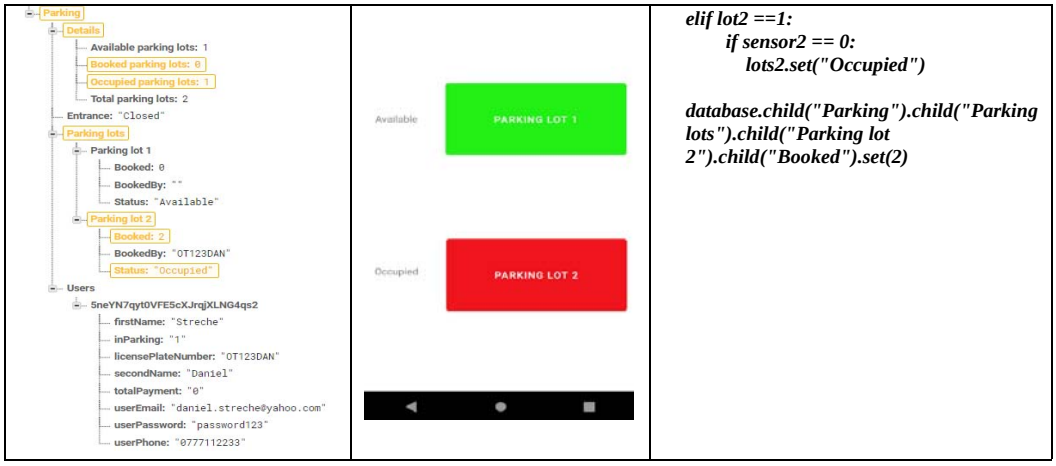

Fig. 9 Updating process in database after the parking lot 2 is occupied

When the mobile phone application retrieves this information from the database, the "REQUEST THE ENTRY CODE" button (Fig. 8), displayed on the cell phone screen, it is replaced by the "PAY AND REQUEST THE EXIT CODE" button (Fig. 10).

3.7. Release of the parking lot

When the driver releases the parking lot, he must open the application on the cell phone and requests the payment and QR code. Otherwise, he has to contact the parking administrator. To remind the driver of the need to request the exit code, a warning message is displayed on the main page of the graphical interface (Fig. 10).

When the parking space is released and the user is authenticated, the payment monitoring method is completed and a message with the total payment amount is displayed. The payment method consists in taking two variables of time i.e. when the user occupied the parking place and the moment when he released it. The mobile application calculates the time between these two variables and multiplies it with the tariff charged by the parking owner.

At the same time, the amount is also recorded in the user's account, and it can be displayed on the account details page. The account details page provides data regarding the account of the authenticated user, such as his full name, the registration number of the car and the total payment for the number of hours he occupied the parking space.

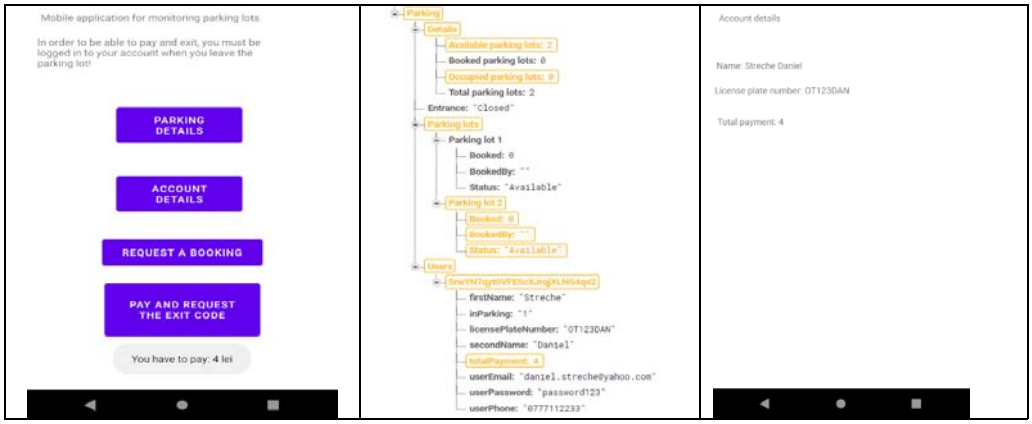

Fig. 10 Updating database when a parking space is released

3.7. Exit of the parking area

To leave the car parking, the user must press the "PAY AND REQUEST THE EXIT CODE" button. This button can only be used if the driver has paid i.e., he has been authenticated when the parking space is cleared. By pressing this button, it will be opened the page that displays the QR code required to exit the parking area (Fig. 11).

Fig. 11 Updating database when leaving the parking area

The user is allowed to exit from the parking area by positioning the QR code located on the mobile phone screen in front of the video camera located at the parking exit. When scanning the QR code, the exit barrier is lifted by the actuator, and it closes after the car has left. After scanning the QR code, the information encrypted in it is decrypted using the decode function from the pyzbar library and transmitted to the database via the Raspberry Pi development board. The information encrypted on QR code is “Open”.

4. Conclusion

In this paper, it is presented a smart parking model based on a Raspberry Pi 3 development board that simulates a real parking using the following components:

- two distance sensors used to check the occupancy and releasing of parking lot;

- a servomotor and a Raspberry Pi video camera used to create a parking entry/exit system.

The designated graphical interface includes and implements several functions that lead to an improved security in car parking, as follows:

- registration and authentication of a new user;
- registration of information regarding the parking status;
- information about user account;
- reservation of parking lot;
- payment method monitoring system;
- method of scanning the QR codes required to enter/exit the car parking.

The total cost of the system presented in this paper is about 100 euros. This is the cost to purchase the electric components.

Using this smart parking system, drivers can save time and money. The information that is provided in real time through the graphical user interface is beneficial for the driver, who can avoid traveling to the fully occupied park.

Also, in addition to information on the status of the car parking received thru the cell phone application, it can be provided information about hourly rate of a car parking.

This system can also help the environment and infrastructure in large cities by improving traffic and it can be implemented for single car parking or large network of car parking. Plus, by implementing a differentiated payment method, users may be charged with different rates depending on the time when the reserved space is occupied and vacated.

And undoubtedly, the smart car parking is the solution to the increasingly congested traffic in major cities and a real solution to reducing the pollution generated by the globally exponential increase of the number of vehicles.

REFERENCES

[1] - Number of passenger cars and commercial vehicles in use worldwide from 2006 to 2015 Disponibil la: URL: https://www.statista.com/statistics/281134/number-of-vehicles-in-use-worldwide/

[2]. - Searching for Parking Costs Americans $73 Billion a Year; Disponibil la URL: https://inrix.com/press-releases/parking-pain-us/

[3] – D. Prochazkova and J. Prochazka, "Smart cities and critical infrastructure," 2018 Smart City Symposium Prague (SCSP), 2018, pp. 1-6, doi: 10.1109/SCSP.2018.8402676.

[4] - R. Hammons and J. Myers, "Smart Cities," in IEEE Internet of Things Magazine, vol. 2, no. 2, pp. 8-9, June 2019, doi: 10.1109/MIOT.2019.8892761.

[5] P. Melnyk, S. Djahel and F. Nait-Abdesselam, "Towards a Smart Parking Management System for Smart Cities", 2019 IEEE International Smart Cities Conference (ISC2), 2019, pp. 542-546, doi: 10.1109/ISC246665.2019.9071740.

[6] – S. Das, A Novel Parking Management System, for Smart Cities, to save Fuel, Time, and Money, IEEE 9th Annual Computing and Communication Workshop and Conference (CCWC), pag. 950-953, 2019.

[7] - C. Recoșeanu, A. S. Deaconu, A. I. Chirilă, V. Năvrăpescu, I. D. Deaconu, C. Ghiță, Remote monitoring of a permanent magnet synchronous motor using android devices, Scientific Bulletin, University POLITEHNICA Bucharest, Series C: Electrical Engineering, vol. 2, 2013.

[8] - S. N. Pandit, R. M. Krishna, R. Akash and M. Moharir, Cloud Based Smart Parking System for Smart Cities, International Conference on Smart Systems and Inventive Technology (ICSSIT), pag. 358-354, 2019.
[9] - Meet Android Studio – De pe developer.android.com, Disponibil la URL: https://developer.android.com/studio/intro
[10] – G. Yan, S. Olariu, M. Weigle, M. Abuelela, SmartParking: A Secure and Intelligent Parking System Using NOTICE, Conference Intelligent Transportation Systems, 2008. ITSC 2008.
[11] – Introduction to Firebase – Disponibil la URL: https://hackernoon.com/introduction-to-firebase-218a23186cd7
[12] – A. Ahad, Z. R. Khan, S. A. Ahmad – Intelligent Parking System, World Journal of Engineering and Technology, Vol.4 No.2, May 2016.
[13] N. B. A. Warif, M. I. S. S. Azman, N. -S. N. Ismail and M. A. Remli, "IoT-based Smart Parking System using Android Application," 2020 Emerging Technology in Computing, Communication and Electronics (ETCCE), 2020, pp. 1-6, doi: 10.1109/ETCCE51779.2020.9350914.
[14] M. Owayjan, B. Sleem, E. Saad and A. Maroun, "Parking management system using mobile application," 2017 Sensors Networks Smart and Emerging Technologies (SENSET), 2017, pp. 1-4, doi: 10.1109/SENSET.2017.8125048.

Nitrates removal from water using ion exchange technologies

Eliminarea nitraților din apă folosind tehnologii de schimb ionic

Alexandru Matei[1], Elena Vulpaşu[2], Gabriel Racoviţeanu[3]

[1]Ph.D. Student, Technical University of Civil Engineering Bucharest, Faculty of Hydrotechnics, Romania
e-mail: *mateialexandru.ioan@yahoo.com*
[2]Conf.dr.chem.eng., Technical University of Civil Engineering Bucharest, Faculty of Hydrotechnics, Romania
e-mail: *vulpasu@utcb.ro*
[3]Prof.dr.eng., Technical University of Civil Engineering Bucharest, Faculty of Hydrotechnics, Romania
e-mail: *gabriel.racoviteanu@utcb.ro*

DOI: 10.37789/rjce.2022.13.4.2

Abstract. During the last decades, ion exchange materials technology has evolved from laboratory to industrial use with significant technical and commercial impact. The goal of this paper is to briefly review the ion exchange technologies used for nitrate removal from water intended for human consumption. The following information will be provided: a brief history of ion exchangers, design considerations, process considerations, advantages, disadvantages, process performance, costs and examples of water treatment plants across the Globe that use ion exchangers technology for nitrate reduction. Also, the experimental results regarding the influence of competitive ions on the nitrogen ion retention efficiency on a specialized ion exchange resin will be presented.

Keywords: Ion exchange, Nitrates, water treatment, Pollution

1. Introduction

Nitrogen compounds in natural waters (surface or groundwater) exist in several forms, depending on the level of pollution and depending on the presence or absence of oxygen.

The forms under which nitrogen compounds appear in water are molecular nitrogen, organic nitrogen, ammoniacal nitrogen, nitrates and nitrites.

High concentrations of nitrates in water can result from direct water pollution such as pollution from agriculture through intensive use of nitrogen-based fertilizers or indirectly through the release of organic substances that release nitrogen compounds in a lower state of oxidation by decomposition, which then, through bacterial oxidation, leads to the formation of nitrates.

Normally, the concentration of nitrogen compounds in surface waters is low, ranging from 0-18 mg/l, but can reach much higher values in the case of farms, industrial discharges or discharges of insufficiently treated wastewater. Also, the concentration of nitrates can fluctuate seasonally.

In most European countries, the concentration of nitrates in raw water has gradually increased in recent decades.

The concentration of nitrates present in groundwater is dependent on the geology of the aquifer. In the case of waters containing nitrates of natural origin, the recorded concentrations do not have values higher than 4-9 mg/l. In the case of aquifers located in areas where intensive agriculture is practiced, the nitrogen concentrations recorded can reach hundreds of milligrams per liter. For example, in agricultural areas in India, values of 1500 mg/l have been recorded [1].

Nitrogen compounds endanger human health. Nitrates ion is a less dangerous form for adults, but for newborn's, it can cause methemoglobinemia - "blue baby syndrome". Nitrates as such are not toxic, for becoming dangerous to the newborn's body, they must be converted into nitrites. Once in the blood, nitrites combine with hemoglobin, forming methemoglobin, which creates an oxygen deficiency in the body. Methaemoglobin is oxidized and cannot act as a carrier of oxygen in the blood.

Nitrites are formed by the reaction of nitrate with saliva in most cases. In infants under one year of age, however, the relatively alkaline conditions in the stomach allow bacteria to form nitrites. Up to 100% of ingested nitrate is reduced to nitrite, compared to 10% in adults and children over one year of age.

Nitrosamines and nitroamides are formed when nitrates or nitrites are administered with nitrosatable amines, such as amino acids in proteins. However, epidemiological studies, mainly on gastric cancer, have not yielded consistent results. Studies on the carcinogenic effect of nitrates are currently being reviewed.

A balanced diet, adequate in vitamin C, can partially protect against the effects of nitrate–nitrite intake [2].

In Romania, the maximum allowable limit for nitrates in drinking water is 50 mg/l, according to law 458/2002 [3], the same value that is recommended by the World Health Organization (WHO, 2011). Also, the 2184/2020/EU Directive impose a maximum allowable concentration of 50 mg/l for nitrates in water intended for human consumption. According to the EPA, the maximum allowable limit for nitrates in drinking water is 10 mg N/l.

2. Nitrates removal technologies

As stated, an increase in nitrate concentrations of water is observed worldwide. Over time, several methods have been developed to reduce the concentration of nitrates in water for human consumption. The main treatment processes applicable to sources that exceed nitrates are:

- Biological processes – are based on the development of a specific biomass. For maintaining it, a food source must be added, usually methanol, increasing the concentration of total organic carbon and the risk of the formation of THM, in case of chlorine use for disinfection, which are susceptible of being carcinogenic. The process must be controlled rigorously, is very sensitive to inhibitory substances, the initiation of the process with biomass recovery takes about a month and if the biomass is lost, the process must be stopped during its regeneration [4];
- Reverse osmosis - is a physical process that involves forcing the water through a semipermeable membrane. The process takes place at high pressure levels, higher than the osmotic pressure, leading to a high energy consumption. From the process results ultrapure water (65% and 80%) and concentrate (20% -35%), regardless of the quality of raw water. The main problem is the concentrate, which must be treated, and managed properly [5.6];
- Electrodialysis - is suitable for low flows. Electrodes are inserted into the volume of water and a direct or alternating current is applied between the electrodes, thus leading to water electrodialysis [7, 8];
- Ion exchange - the process is relatively stable, but it can only work automated because the concentration of nitrates in the effluent is variable over a cycle, increasing progressively with the reduction of exchange capacity. For denitrification, masses of ion exchangers are especially dedicated to nitrate retention.

2.1 Ionic exchange

Ion exchange is a reversible reaction in which a target ion in the aqueous phase is transferred to a solid phase and exchanged with a like-charged ion that diffuses into solution [9].

Usually, the process is used for water softening, where calcium, magnesium and other polyvalent cations are exchanged for sodium [10]. The technology has high treatment capacity, high removal efficiency, fast kinetics and can be utilized for water reuse, which has a significant economic importance [11].

In water treatment plants, ion exchange is also used to remove specific contaminants such as nitrate, arsenic and radium [10].

2.1.1 Types of ion exchangers

In general, any water-soluble ionic compound has the property of ion exchange. Ion exchangers can be:

- Organic ion exchangers;
- Mineral ion exchangers.

Mineral ion exchangers were the first substances used for the ion exchange process. They are called zeolites and their general formula is:

$$Me_{2/x}O \cdot Al_2O_3 \cdot nSiO_2 \cdot mH_2O \text{ [7].} \quad (1)$$

Although inorganic ion exchange materials were first to be recognized, they lost their utility after the discovery of organic resins due to their relatively low ion exchange capacity and chemical instability. Zeolites have been gradually replaced by synthetic resins due to their faster exchange rates, longer life and much higher treatment capacity. Currently, ion exchange resins are used. They consist of two main structural components: the resin support and the functional groups that participate in the ion exchange process.

The resin support has to maintain the mechanical and chemical stability. The functional groups have an acidic or basic character that can be strong or weak and ensure the electrostatic interaction with ions of opposite sign in the proximity. They react both with ionic species in their vicinity and with neutral molecular species, such as water, through ion-ion or ion-dipole interactions [6, 7, 10].

Ion exchange resins can be found in two forms, in the form of gel and macroporous or poorly crosslinked. Their structure is practically identical, in both cases, they are obtained by copolymerization, the difference between them is given by the porosity.

Gels have a natural porosity that results from the polymerization process and is limited to the distance between the molecules that make up the gel. Macroporous resins have a high porosity resulting from their artificial growth by using substances specially created for this purpose. These resins have larger channels called macropores that have a higher capacity to absorb organic substances [5]. An ion exchange resin consists of a three-dimensional, cross-linked polymer matrix of hydrocarbon chains carrying fixed ionic groups, the electric charge of which is compensated for by mobile ions of opposite charge (“counterions”). The usual matrix is polystyrene crosslinked with divinylbenzene of 3 to 8%, to provide structural stability.

Counter ions are free to diffuse. When the resin comes in contact with an electrolyte solution, the resin takes up the solvent and some additional mobile ions that have the same charge sign as the fixed ionic groups.

In the process, the counter ions present initially in the resin are replaced by another species of ions.

2.1.2 Properties of Ion Exchange Resins

The most important properties of resins are exchange capacity, selectivity and structural stability.

Exchange capacity – the quantity of counterions that can be exchanged onto the resin is one of the major considerations when selecting an ion exchange resin [10].

The exchange capacity is a measure of how many ions the resin can capture per unit volume [7].

The exchange capacity can be reported as milliequivalents per gram of dry resin or milliequivalents per millilitre of wet resin. The typical dry-weight capacity of a strong resin is situated in the range of 3.6 to 5.5 meq/g [10].

Selectivity – Ion exchange resins have a variable affinity for the ions in solution. Selectivity can be expressed as a selectivity coefficient (Kji) where "I" represents the cation (or anion) and "j" represents the exchanged ion. The greater the selectivity coefficient is, the greater is the preference for the ion by the exchange resin. For process design considerations, usually, separation factors are used rather than selectivity coefficients. The separation factor is a measure of the preference of one ion for another ion and can be expressed as:

$$a_j^i = \frac{Y_i X_j}{X_i Y_j} \qquad (2)$$

Where:
a_j^i= separation factor;
Yi= resin phase equivalent fraction of counterions;
Xj= equivalent fraction of presaturant ion in aqueous phase;
Yj= resin phase equivalent fraction of saturated ions;
Xi= equivalent fraction of counterion in the aqueous phase. [10]

Structural stability and Service life – a lot of issues can occur in the operation of ion exchangers technology like resin bead compression that can lead to inadequate liquid distribution and reduced flow, swelling, shrinking, oxidation of the resin beads, etc.

Some of these issues can be avoided by selecting an appropriate resin, based on the quality of the raw water and selecting a proper pretreatment process [10].

2.1.3 Process operation

Commonly, the following steps are used in an ion exchange cycle:

1) Service – The raw water is passed through the ion exchange unit until the effluent is exceeding the designed limit of the pollutant intended for treatment. The unit is then taken out of service for the regeneration of the resin.

2) Backwash – water is introduced in the unit and it flows up through the bed until it is expanded by 50 percent. This step is used for removing any suspended solids that have accumulated through the cycle.

3) Regeneration - is a process that involves removing retrained ions from the in-service service from the fully loaded resin beads so the resins can be reused. It can be regenerated using a high concentration of salt or other regenerant chemical compound [12]. Depending on the flow direction of the regeneration solution, there are two methods:

- Co-current regeneration - the regenerating substance flows in the same direction as depletion;
- Counter current regeneration - the regeneration solution flows in the opposite direction to the depletion of the resin.

Co-current regeneration consists in bringing the concentrated solution with A ions in contact with the upper layers of the exchanger, saturated with B ions. They migrate into the lower layers of the resin (not yet exhausted) that can capture B ions. Total regeneration, the resin assumes a double ion exchange process. [5]. If the amount of regeneration solution is limited, the B ions will not be completely removed from the exchangers, and the lower layers will not be completely regenerated, leading to a shorter operating time than in the previous cycle and / or a quality weaker treated water than the previous cycle. The following figure schematically shows the co-current regeneration process of ion exchange resins.

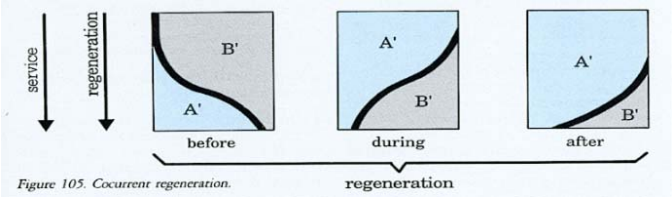

Figure 1. Co-current regeneration [5].

Counter current regeneration is different from co-current regeneration by the way of introducing the concentrated solution. Thus, counter current regeneration consists in bringing the concentrated solution with A ions in contact with the lower layers of the exchanger, unsaturated with B ions. In this case, B ions will be eliminated more easily because they cannot be regenerated in the already depleted layers and thus ensure a higher volume of regenerated resin that can be used in the next cycle, compared to current regeneration [5].

In conclusion, counter current regeneration confers a much higher efficiency in terms of the amount of resin regenerated compared to co-current regeneration [5].

The main advantages of counter current regeneration are:

- high efficiency and low amounts of reagent;
- better quality of treated water because the lower layers are regenerated with a larger amount of regenerating solution.

The following figure schematically shows the counter current regeneration process of ion exchange resins.

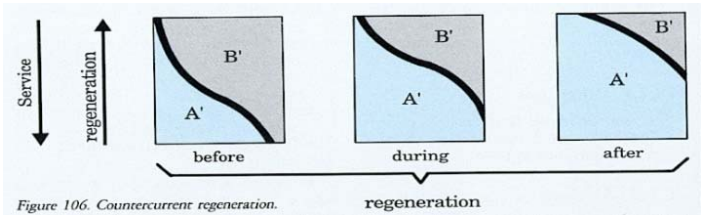

Figure 2. Counter current regeneration [5].

4) Slow rinse – Rinse water is passed through the unit using the same flow direction as the regenerating flow rate for pushing the regenerating chemicals through the bed.

5) Fast rinse – Final rinse step, consists of rinse water at the same flow as the service flow rate for removing any remaining regenerating solution.

6) Return to service.

The following figure presents a typical ion exchange unit.

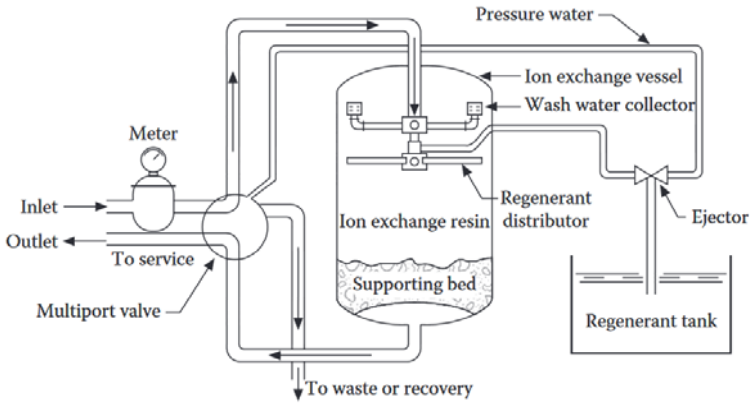

Figure 3. Typical ion exchange unit [13].

2.1.4 Brine disposal

The solution resulting from regeneration, which contains high concentrations of salt and ammonium, is a waste that can create complications in management because it is hardly accepted in a treatment plant. For small household units, it has an insignificant impact on the wastewater treatment plant but for larger municipal systems, the problem is much more significant.

The alternative solutions for the evacuation of brine resulting from regeneration are the evacuation in the seas and oceans, the injection in deep wells and their use as fertilizer (depending on the substances dissolved in the regeneration solution). The solution for brine disposal is site-specific and has to be considered very early in the design process because it can be very expensive.

2.1.5 Ion exchangers used for nitrate removal

Now, ion exchange is the most used method for the removal of nitrate in potable water treatment.

The process involves passage of nitrate loaded water through a resin bed that contains a strong base anion exchange resin on which nitrate ions are exchanged for chloride until the resin is exhausted [14].

The relative order of affinity for the three most common ions in drinking water compared to nitrates is Sulphate > Nitrate > Chloride > Bicarbonate [15]

2.1.6 Design consideration

There are various tools used for assisting ion exchange design, like CADIX and Ion Exchange calculator [7].

The key considerations in the application of ion exchange to nitrate removal, according to California's State Water Resources Control Board – Drinking water treatment for nitrate are presented in the next table:

Table 1.

Summary of design considerations for conventional ion exchange [7].

Applications	Main considerations
Resin Selection	• Generic SBA resins for maximum exchange capacity (for low sulfate) o Less expensive than nitrate selective resins o Less frequent regeneration due to higher capacity (in the absence of co-contaminants) o Nitrate dumping potential •Generic SBA resins for maximum exchange capacity (for low sulfate) o Less expensive than nitrate selective resins o Less frequent regeneration due to higher capacity (in the absence of co-contaminants) o Nitrate dumping potential •Nitrate selective resins to avoid nitrate dumping (for high sulfate) o More expensive than generic resins o Longer bed life o More nitrate removed per unit of waste brine
Pretreatment	•Filtration to remove iron, manganese, TSS, and organic matter to prevent resin fouling •Water softening (antiscalant, acid, or water softener) to prevent scaling •Dichlorinations to prevent resin oxidation
Post-Treatment	•Chloride: alkalinity ratio •Chloride: sulfate ratio and galvanic corrosion •Potential: pH adjustment and restoration of buffering capacity to avoid corrosion
Chemical Usage	• pH adjustment (caustic soda or soda ash) • Regenerant brine, salt consumption
O&M	•Frequency of regeneration depends on water quality and resin type •Fresh brine preparation and waste disposal •Resin loss and replacement: 3 – 8 years lifetime

Applications	Main considerations
	•Continuous or frequent monitoring of nitrate levels •Backwashing to dislodge solids
System Components	•Fixed bed versus continuous regeneration •Key system configuration parameters are system flow rate, bed swelling, bed depth, backwash flow rate, and rinse requirements o Vessels in parallel or in series o Co-current or counter-current regeneration
Waste Management and Disposal	•Significant cost of waste brine disposal is of greatest concern for inland systems •Close proximity to coastal waters is beneficial for brine disposal •Management options can include sewer or septic system, drying beds, trucking offsite, coastal pipeline, deep well injection, and advanced treatment •Disposal options can be limited by waste brine water quality (e.g., volume, salinity, metals, and radionuclides) •Optimization of recycling and treatment of waste brine is desirable.
Limitations	•Need to manage resin fouling o Hardness, iron, manganese, suspended solids, organic matter, and chlorine •Competing ions (especially sulfate) •Disposal of waste brine •Possible role of resin residuals in DBP formation

2.1.7 Treatment plants that use ion exchangers for nitrate reduction

The reduction of nitrate from water supply sources by means of ion exchangers began in France in 1985. Since 1989 there are 6 treatment plants with ion exchangers in operation with flow values ranging between 10 m³/h and 600 m³/h.

Technologies of ion exchange-based denitrification have been developed in France and include the AZURION, ECODENIT and NITRACYCLE systems [6].

The ECODENIT system
It was developed by OTV and is used for nitrate reduction at the treatment plant of Binic, a locality situated in the western region of France.

The treatment plant treats a flow of 160 m³/h, the source being surface water with a concentration of nitrate ranging from 45 to 100 mg NO3-/ l, with a maximum value of 165 mg NO3-/l.

The plant consists of three beds with ion exchangers, each containing 2700 l of natural resin Dowex SRBP. Before entering in the ion exchange step, the water is pretreated using a unit of coagulation, decantation and filtration.

After the process, 75% of the nitrates are reduced, along with 90% of sulphate ions and 30% of bicarbonates.

The brine which results after regeneration is transported to the nearest wastewater treatment station that accepts it. The volume of brine is approximately 55 m³/day and it contains 450 kg/day NO3- and 516 kg/day Cl- [6].

The same system is used in Pleven, another locality from France. The raw water has a concentration of 70 mg/l of nitrate. In the treatment process, only a part of the whole volume of raw water is treated by ion exchangers. The treated water is blended with raw water so that the resulting nitrate concentration is below 25 mg/l [6].

The NITRACYCLE system

It was developed by S.A.U.R. (Société d'Aménagement Urbain et Rural) – a French group operating in the water sector, whose main activity is the delegated management of services to local authorities and is a major player in the market of engineering and construction related to water treatment [16].

In this process, a macroporous resin is used to reduce nitrates in the water. The process consists of repeated operating cycles in the following order: treatment, prewash, regeneration and washing. Regeneration is performed counter current.

The used regenerant is usually discharged into the local sewer system. The brine generally contains sodium (15 g/l), chloride (13 g/l), nitrate (12 g/l) and sulphate (5 g/l). Since 1990, eight NITRACYCLE systems have been in operation; 6 for drinking water sources and 2 for the treatment of water used in the food industry. Drinking water treatment plants are located in France. Their characteristics are presented in the following table.

Table 2.

Nitracycle treatment plants [6].

Treatment plant	Capacity (m^3/h)	Nitrate (mg/l)		Efficiency
		Raw water	Effluent	
Plounevez – Lochrist	50	120	25	79%
Grez en Bouere	60	70	35	50%
Souppes sur Loing	120	60	25	58%
Ballee	60	80	25	69%

The Azurion system

It was developed by Degremont and it is used in Ormes-sur-Voulzie, near Paris and Plouenan, Brittany. Both were commissioned in 1987.

The Ormes-sur-Voulzie treatment plant has a capacity of 27 m^3/h. The average concentration of nitrates in raw water is 60 mg/l. After the treatment process, the amount of nitrates in effluent doesn't exceed 25 mg/l.

The Plouenan treatment plant has a capacity of 600 m^3/h. Raw water comes from a surface source. The average concentration of nitrates is 80 mg/l. During the treatment process, only a part of the volume is treated by ion exchange. The treated water is then blended with raw water (that by-passed the ion exchange unit), resulting in a concentration below 25 mg/l nitrates in distributed water. The solution resulting from regeneration is discharged in the sea.

For both treatment plants, the countercurrent regeneration is used for regeneration [6].

In the USA, there are 12 treatment plants in which ion exchange is used for denitrification. The flow values are ranging between 7.4 m³/h (Ellsworth, Minnesota) to 1,577 m³/h (Des Moines, Iowa) [7].

The city of Ohio treatment plant

The City of Ohio public works operates a groundwater source impacted by nitrate pollution. The amount of nitrate in raw water is ranging between 40 and 100 mg/l. The water also contains perchlorate. The capacity of the treatment plant is 1,135 m³/h.

Ion exchange and blending are used to address high nitrate and perchlorate levels. Treated water from the Metropolitan Water District of Southern California (3 parts) and treated water from the Chino Basin Desalter Authority (1 part) is used for blending, for achieving a maximum nitrate concentration of 36.3 mg/l in drinking water. The system was commissioned in 2006.

Waste brine is sent to the LA County Sanitation District, with a total disposal cost of 50,000$ per year [7].

Indian Hills

The Indian Hills Water District operates a groundwater well which has a capacity of 12 m³/h. Because the well has historical nitrate concentrations ranging from 12 mg/l to 16 mg/l as N, the District has implemented a countercurrent ion exchange that uses a Magnetic Ion Exchange resin in a series of fluidized beds which reduce the brine generation.

The magnetized resin encourages agglomeration of loaded resin particles and a faster settling. The loaded resin is removed from the bottom of the Ion exchange unit and it is passed to regeneration. Regenerated resin is continuously added to the top of the unit. Using this configuration, the risk of nitrate spiking is reduced. Also, the competing ions, like sulphate can be removed early on the resin vessel. Regeneration is performed continuously in small batches, the number of regenerations per day depends on the system's flow rate.

The waste brine is stored in an underground storage tank. Periodically, the brine is pumped from the tank and it is land applied [7].

3. Materials and methods

The experimental trials were performed on two samples of synthetic water prepared from distilled water in which NO3-, SO42-, HCO3- ions were added, using different concentrations so the influence of ions that compete with the nitrate ion in the ion exchange process can be highlighted.

Table 4.

Characteristics of synthetic water.

No.	Item	U.M.	Sample 1	Sample 2
1	NO_3^-	mg/l	100	100
2	KNO_3	mg/l	163	163
3	SO_4^{2-}	mg/l	130	165
4	K_2SO_4	mg/l	181	271
5	HCO_3^-	mg/l	103.7	201.3
6	$NaHCO_3$	mg/l	138	276
7	pH	mg/l	9.1	8.6

The A520 E Purolite ion exchange resin was used to perform the experiment. This is a macroporous resin, strongly basic, which is specially designed to retain nitrates from water.

An installation consisting of glass mini-columns with porous glass drainage was used. 25 ml of resin was introduced into it. The flow rate through the columns was adjusted to 26 ml/min.

The experimental setup is shown in the following figure.

Figure 4. Experimental setup.

After the following volumes of water passed through the column, samples were collected:

- 250 ml (10 BV);
- 1250 ml (50 BV);
- 2500ml (100 BV);
- 5000 ml (200 BV);
- 7500 ml (300 BV).

For every sample, the following ion concentrations were determined: nitrates, bicarbonates, sulphates and chlorides.

The concentration of nitrates and sulphates was measured using a spectrophotometer, HACH DR3900 and the bicarbonates concentration was determined using the volumetric method, according to SR EN 9963-1/2002.

4. Results and discussions

The results showed that in the first phase of the process nitrates and sulphates are retained with great efficiency, reaching concentrations of 2-3 mg/l after passing a volume of water equal to 50 times the volume of resin (50 BV), regardless of their initial concentration. After this threshold, the concentration of nitrates begins to increase slightly, which indicates a decrease in the exchange capacity of the resin. After passing a volume of water equal to 300 BV, the concentration of nitrates in the effluent reaches close to the limit imposed for drinking water (50 mg/l).

The sulphate concentration increases relatively rapidly after the threshold of 50 BV, reaching the initial concentration after 300 BV for the first sample, respectively after 200 BV for the second sample. For the second sample, it is found not only that there is no exchange of the sulphate ion in the water with the chloride ion grafted on the resin but also an elution of it (ratio C/C0> 1).

For the bicarbonates, it was found that there is a retention of them up to half of the initial concentration, followed by a sudden increase in the effluent concentration so that after 100 BV the bicarbonate concentration in the effluent becomes equal to the concentration of the influent.

The following figures show the variations of the concentrations depending on the volume of water passed through the column and the variation of the C/C0 ratio of the volume of water passed through the column expressed in BV.

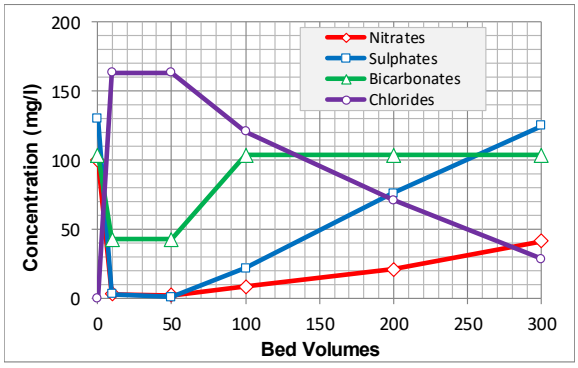

Figure 5. Concentration of indicators depending on the volume of water passed through the column - SAMPLE 1.

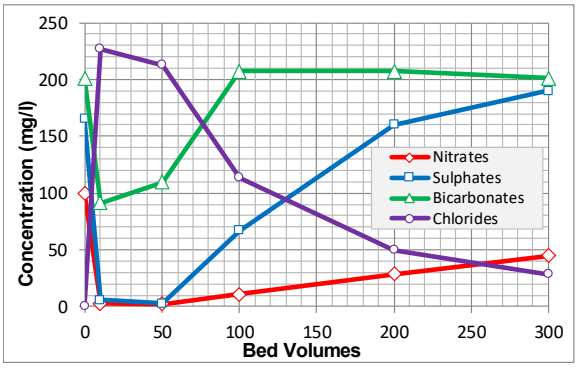

Figure 6. Concentration of indicators depending on the volume of water passed through the column – SAMPLE 2.

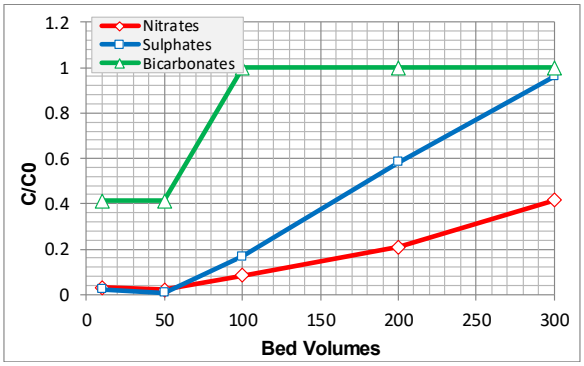

Figure 7. C/C0 variation depending on the volume of water passed through the column - SAMPLE 1.

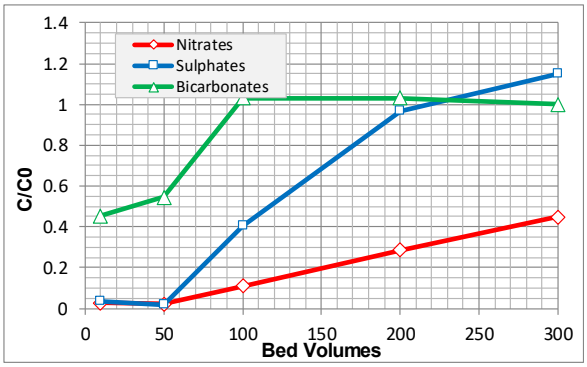

Figure 8. C/C0 variation depending on the volume of water passed through the column - SAMPLE 2.

5. Conclusions

As stated, an increase in nitrate concentrations of groundwater is observed worldwide. The main treatment processes applicable to sources that exceed concentration of nitrates are:

- Biological processes;
- Reverse osmosis;
- Electrodialysis;
- Ion exchangers.

Reverse osmosis and Electrodialysis have good automation possibilities and no need for extensive post treatment but the utility of these processes is limited due to big OPEX costs and the concentrated waste brine which is hard to treat and store [2,17].

The ion exchange process seems to be one of the most suitable treatment technologies for small water systems in terms of nitrate removal because of its effectiveness, simple use, selectivity and relatively low cost [18, 19].

However, the process has several limitations due to the concentration of chlorides in the water because the nitrogen ion in the water is exchanged with the chloride ion grafted onto the anion exchanger. There may be situations in which concentrations of nitrates are reduced but exceedances of chlorides may occur. Also, although anionites have been designed to be selective, there is still a competitive action given by sulphate and bicarbonate ions. Groundwater generally has high concentrations of bicarbonate that, when competing with the nitrogen ion, lead to premature depletion of the anionite's exchange capacity.

When the exchange capacity is exhausted, the anionite mass must be regenerated with significant consumption of regeneration brine and significant quantities of waste brine with high nitrogen content, which represents a difficult waste to be managed.

The process is relatively stable, but one of the drawbacks is that it can only work fully automated because the concentration of nitrates in the effluent is not constant over a cycle, but increases progressively with the reduction of anionite exchange capacity. The process requires permanently qualified operating personnel.

The efficiency of the processes in reducing the amount of nitrates in the water varies in the range of 30-96%.

The main advantages of ion exchange technologies are:

- easy to automate;
- the process can be started in minutes and ensures stable operation, regardless of temperature;
- can treat the whole flow or just a part of it, depending on the flow rate and the concentration of nitrates in it.

The main disadvantages of this technology are:

- waste brine is hard to be managed;
- the corrosivity and the aggressiveness of the water may increase due to the replacement of the bicarbonate and sulphate ions in the water;
- expensive technology if it is used to treat the entire flow in the treatment plant.

In terms of costs, they vary depending on the concentration of nitrogen and other pollutants in the raw water. An estimate of the costs involved in using this technology is presented in the following table.

Table 3.

Costs of ion-exchange technologies [6].

Investment cost ($/m³)	**Operation cost ($/m³)**	**Waste storage ($/m³)**	**Total ($/m³)**
0.06-0.31	0.12-0.2	0.01-0.08	0.18-0.57

The experimental results highlighted the following:

- the nitrate ion can be retained with high efficiency (higher than 95%);
- although the resin used is specially designed for nitrate retention, high efficiency retention of sulfates and bicarbonates has been recorded, which leads to a premature depletion of the resin's exchange capacity;
- the chloride ion is released in solution proportional to the amount of ions retained. In the first phase of the ion exchange process, when the exchange efficiency is very high, if the salt concentration of the water is high, the chloride concentration may increase and exceed the allowed limit for drinking water (250 mg / l according to Law 458/2002);

– It was found that the effluent of the ion exchange columns does not have a constant quality. Careful monitoring of the process is required for all ions involved. This can be a disadvantage if only a part of the raw water is treated using ion exchange technology;

The main conclusion of the experiment is that the ion exchange process for nitrate retention is efficient and can be applied in water treatment for drinking, especially in the case of water with low concentrations of sulfate ions and low alkalinity. Another indicator that limits the application of the process is the concentration of chlorides that will increase proportionally with the amount of nitrate, sulfate and bicarbonate ions retained.

In conclusion, due to the fact that biological denitrification processes are strongly influenced by temperature and reverse osmosis and electrodialysis processes involve high energy consumption, ion exchange is a feasible process for treating water with nitrogen concentrations above the allowable limit for drinking water.

References

[1] Jacks, G., Sharma, V.P. (1983) „*Nitrogen circulation and nitrate in groundwater in an agricultural catchment in Southern India"*, Geo 5, 61–64. DOI: 10.1007/BF0238109

[2] J.J. Schoeman, A. Steyn (2003) „*Nitrate removal with reverse osmosis in a rural area in South Africa",* Desalination, 155, 15-26. DOI: 10.1016/S0011-9164(03)00235-2

[3] Romanian Government - *„Law no. 458/2002"*

[4] O. N. Letimela (1993) *Denitrification of groundwater for potable purposes*, WRC Report, 403

[5] Degremont Water and the Environment (1991) *Water Treatment Handbook*, 6, Rueil-Malmaison Cedex, Paris

[6] Calin, C. (2011) *Procese si Tehnologii pentru Controlul Continutului de Azot din Apa*. Doctoral thesis, Technical University of Civil Engineering of Bucharest.

[7] V. B. Jensen, J. L. Darby, C. Seidel, C. Gorma (2012) *Drinking Water Treatment for Nitrate*- Technical Report, 6

[8] Romanian Ministry of Health, National Institute of Public Health (2012) *Fountain water: Nitrate contamination and methemoglobinemia*, Carol Davila University Publishing House, Romania

[9] F. Helfferich (1995) *Ion Exchange,* Dover Publications, Inc., New York

[10] Mackenzie L. D. (2020) "*Water and Wastewater Engineering, Design Principles and Practice"*, 2, McGraw Hill, USA

[11] Akieh, M. N. et al. (2008) *Preparation and characterization of sodium iron titanate ion exchanger and its application in heavy metal removal from waste waters,* Journal of Hazardous Materials. DOI: 10.1016/j.jhazmat.2007.07.049

[12] https://www.purolite.com/index/Company/Resources/ion-exchange-resin-glossary/what-is-regeneration - last accesed on 7th of October 2021

[13] Anthony M. W. (2016) *Fundamental Principles and Concepts of Ion Exchange*, Environmental Ion Exchange, Principles and Design CRC Press

[14] M. Nujić, D. Milinković, M. Habuda-Stanić *(2017) Nitrate removal from water by ion exchange*, Croatian Journal of Food Science and Technology, 9, 182-186. DOI: 10.17508/CJFST.2017.9.2.15

[15] F. J. DeSilva (2003) *Nitrate removal by ion exchange*, Resintech Inc

[16] https://www.saur.com/en/the-group/history/- last accesed on 13th of October 2021

[17] S. Samatya, N. Kabay, Ü. Yüksel, M.f Arda, M. Yüksel (2006) *Removal of nitrate from aqueous solution by nitrate selective ion exchange resin,* Reactive and Functional Polymers, 66, 1206-1214. DOI:10.1016/j.reactfunctpolym.2006.03.009

[18] M. Dehghani, A. B. Haghighi, Z. Zamanian (2010) *The Efficiency of Amberjet 4200 Resin in Removing Nitrate in the Presence of Competitive Anions from Shiraz Drinking Water,* Pakistan Journal of Biological Sciences, 13, 551-555. DOI: 10.3923/pjbs.2010.551.555

[19] M. Boumediene, D. Achour (2004) *Denitrification of the underground waters by specific resin exchange of ion,* Desalination, 168, 187-194. DOI:10.1016/j.desal.2004.06.186.

Simplified procedure for evaluating energy performance of heat pumps. Energy and economic analysis

Procedura simplificată de evaluare a performanței energetice a pompelor de căldură. Analiza energetica si economica

Florin Iordache[1], Mugurel Talpiga[2]

[1,2] Universitatea Tehnică de Construcţii Bucureşti
Bd. Lacul Tei nr. 122 - 124, cod 020396, Sector 2, Bucureşti, România
E-mail: *fliord@yahoo.com, talpiga.mugurel@gmail.com*

DOI: 10.37789/rjce.2022.13.4.3

Abstract: The use of heat pumps to solve energy issues in the field of thermal utilities in buildings is increasingly recommended and necessary.

Key-words: heat pump, correlation, energy issue

1. Introduction

The use of heat pumps to solve energy issues in the field of thermal utilities in buildings (space heating, preparation of hot water for consumption) is increasingly recommended in the current context in which we talk about nZEB buildings. In this sense, it was an important issue to choose the appropriate capacity of the heat pump in relation to the capacity of the customer served. In this sense, it was considered a space heating type consumer and an air-water type heat pump through which the consumer heating installation was supplied. The correlation between the energy capacities of the consumer and the heat pump is a rather complex problem that involves a number of operating parameters such as the size of the heating system, the temperature range for the heating period and others. In this paper we intend to present mainly the analysis procedure that leads to the identification of the optimal ratio between the energy capacities of the consumer and the heat pump.

2. Description of a new procedure, simplification of the evaluation of the energy performance of the heat pump serving a consumer

The procedure is based on the correlation that exists between the CARNOT refrigeration efficiency and the difference between the hot and cold medium temperatures to which thermal power is delivered and respectively from which thermal power is extracted.

$$\varepsilon_{VP}^{C} = \frac{T_{VP}}{T_{CD} - T_{VP}} = \frac{\theta_{VP} - \Delta t_{VP} + 273.15}{\theta_{CD} - \theta_{VP} + \Delta t_{CD} + \Delta t_{VP}} \quad (1)$$

A graphical representation of the CARNOT refrigeration efficiency according to relation (1) can be found in fig.1 which follows:

For values of the average temperature differences at the evaporator and condenser of the heat pump of approx. 5 oC a fairly good correlation is obtained between the efficiency of εCVP and the temperature difference Δθ = θCD - θCD as can be seen from fig. 2.

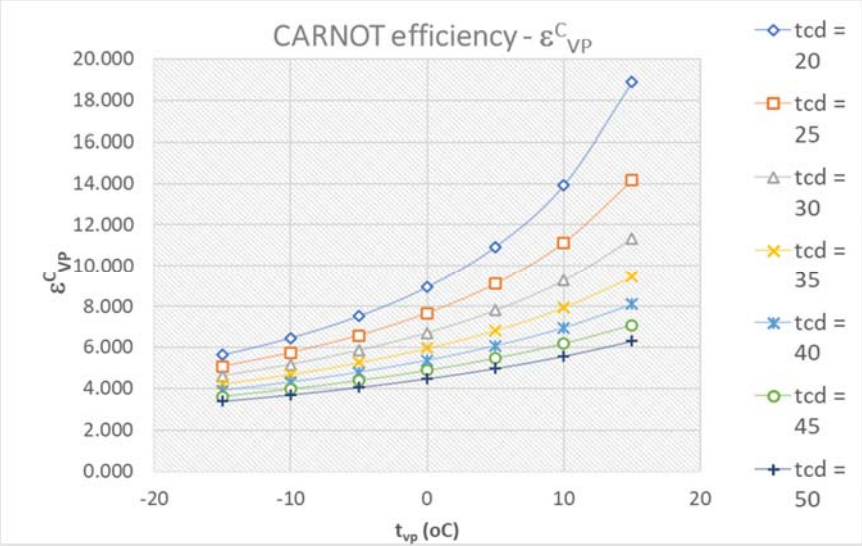

Fig.1

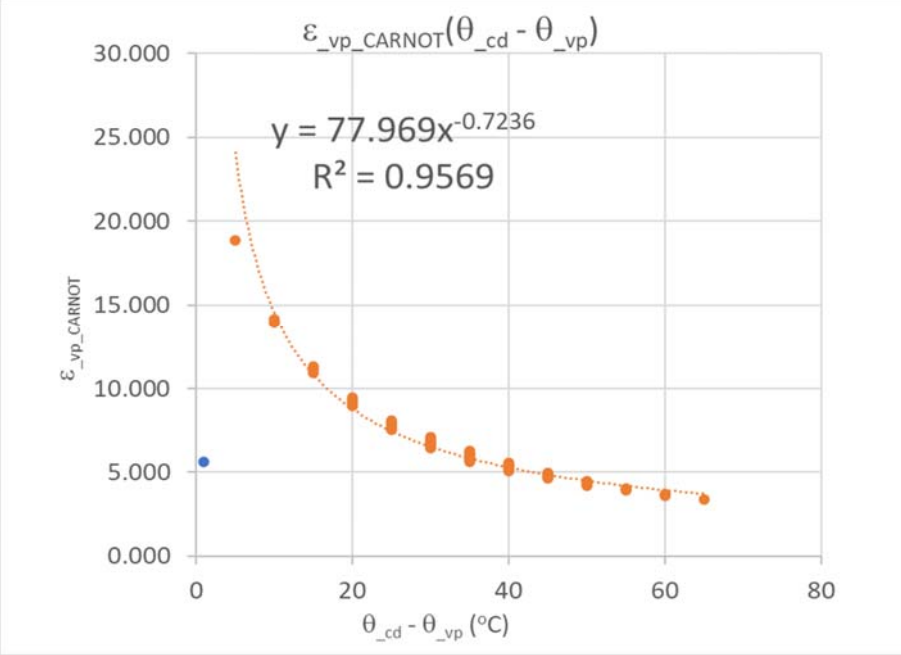

Fig. 2

Which means:

$$\varepsilon_{VP}^{C} = 77.969 \cdot \Delta\theta^{-0.7236} = \frac{77.969}{\Delta\theta^{0.7236}} \tag{2}$$

Considering the correlation between isentropic refrigeration efficiency and CARNOT refrigeration efficiency highlighted in several previous works [1], [2], [3].

$$\begin{aligned} \varepsilon_{VP}^{IZ} &= M \cdot \varepsilon_{VP}^{C} - N = 0.958 \cdot \varepsilon_{VP}^{C} - 1.5321 \\ \varepsilon_{VP}^{IZ} &= 0.958 \cdot \frac{77.969}{\Delta\theta^{0.7236}} - 1.5321 \end{aligned} \tag{3}$$

The result is the coefficient of performance of the heat pump, COP expression:

$$\begin{aligned} COP &= \left(1 + \varepsilon_{VP\_iz}^{*} \cdot \eta_{iz}\right) \cdot \eta_{EL} \\ COP &= \left[1 + \left(0.958 \cdot \frac{77.969}{\Delta\theta^{0.7235}} - 1.5321\right) \cdot \eta_{iz}\right] \cdot \eta_{EL} \end{aligned} \tag{4}$$

The effective evaluation of the COP presupposes the knowledge or the prior determination of the isentropic, η_{iz} and electrical η_{EL} yields.

On the other hand, in terms of electric power, we have the expression:

$$P_{EL} = \frac{P_{CD}}{COP} \tag{5}$$

If the heat pump is chosen so that Pcd = Pnec, and:

$$\begin{aligned} P_{nec} &= H \cdot \left(t_{i0} - t_e\right) \\ P_{CD} &= H \cdot \left(t_{i0} - t_e\right) \end{aligned} \tag{6}$$

On the other hand, according to the working procedure presented in detail in [4], the temperatures of the cold and hot media are established according to:

$$\begin{aligned} \theta_{VP} &= t_e \\ \theta_{CD} &= \frac{t_{m0} - t_{e0}}{t_{i0} - t_{e0}} \cdot t_{i0} - \frac{t_{m0} - t_{i0}}{t_{i0} - t_{e0}} \cdot t_e \\ t_{m0} &= \frac{1}{2} \cdot \left(t_{T0} + t_{R0}\right) \end{aligned} \tag{7}$$

Relation (7_2) considers the qualitative thermal regulation which presupposes adequate values of the temperatures of the thermal agent in the central heating installation of the consumer with external temperature.,

With notation:

$$a = \frac{t_{m0} - t_{i0}}{t_{i0} - t_{e0}} \tag{8}$$

Equations (7) are redraw as:

$$\begin{aligned}
&\theta_{VP} = t_e \\
&\theta_{CD} = (1+a)\cdot t_{i0} - a\cdot t_e \\
&\Delta\theta = \theta_{CD} - \theta_{VP} = (1+a)\cdot(t_{i0} - t_e)
\end{aligned} \tag{9}$$

Thus, there are relations between the electric power and the thermal power emitted at the capacitor:

$$\begin{aligned}
&P_{EL} = \frac{P_{CD}}{COP} = \frac{P_{CD}}{\left[1+\left(0.958\cdot\frac{77.969}{\Delta\theta^{0.7236}} - 1.5321\right)\cdot\eta_{iz}\right]\cdot\eta_{EL}} \\
&P_{CD} = P_{EL}\cdot COP = \left[1+\left(0.958\cdot\frac{77.969}{\Delta\theta^{0.7236}} - 1.5321\right)\cdot\eta_{iz}\right]\cdot\eta_{EL}\cdot P_{EL} \\
&\Delta\theta = (1+a)\cdot(t_{i0} - t_e)
\end{aligned} \tag{10}$$

If we consider the dependence of the thermal power necessary for the consumer and of the thermal power delivered by the condenser of the heat pump depending on the external temperature presented in the relations (11):

$$\begin{aligned}
&P_{nec} = H\cdot(t_{i0} - t_e) \\
&P_{CD} = P_{EL}\cdot COP = \left[1+\left(0.958\cdot\frac{77.969}{\Delta\theta^{0.7236}} - 1.5321\right)\cdot\eta_{iz}\right]\cdot\eta_{EL}\cdot P_{EL} \\
&\Delta\theta = (1+a)\cdot(t_{i0} - t_e)
\end{aligned} \tag{11}$$

These can be represented graphically as seen in fig. 3.

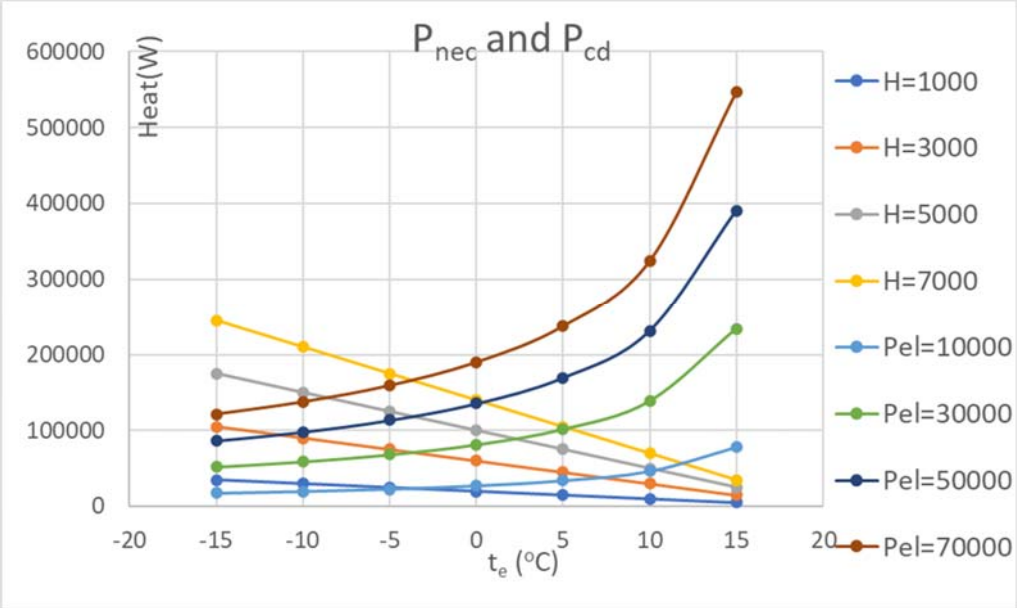

Fig. 3

Both from relations (11) and from fig.3 it is observed that each of the 2 families of curves depends on a parameter, Thus the necessary thermal power of the consumer depends on the thermal capacity of the heated building, H, and the thermal power delivered by the condenser heat pump depends on the electrical supply power of the heat pump compressor. In fig. 2 it is observed how the 2 families of curves intersect in points characterized on the abscissa of external equilibrium temperature. We consider that there is an optimal association between the curves of the 2 families. Each line in the required power beam $P_{nec} = P_{nec}(t_e, H)$ has its optimal pair curve in the $P_{cd} = P_{cd}(t_e, Pel)$ beam. This curve, the optimal pair, will result from an energetic and economic analysis.

For this analysis, a value was chosen for the heat transfer capacity of the consumer, H = 5000 W / K, which corresponds approximately to a 10-storey household. Next, we looked for in the bundle of power curves delivered by the heat pump those curves that intersect the line corresponding to the consumer power for H = 5000 W / K at the points of external equilibrium temperature, t_{eE} = -15, -10, -5, 0 , +5 and +10℃. In addition, it will be considered that these values of external temperature are representative (averages) on domains of 5℃ and on the whole cold period of the year they have durations as it results from tabel 1.

Tabel 1

t_{eE} (oC)	Δte (oC)	Nz (zile)
-15	-17.5 …-12.5	2
-10	-12.5 …-7.5	11
-5	-7.5 …-2.5	32
0	-2.5 …+2.5	60
5	+2.5 …+7.5	53
10	+7.5 …+12.5	24

What needs to be done is to find the electrical power parameter from the corresponding expression of the thermal power delivered by the heat pump in case its vapor becomes equal to the required thermal power of the consumer for the external equilibrium temperatures t_{eE} = -15, -10, -5, 0, +5 and +10 oC. Solving is simple using relationships (11). The values presented in table 2 are obtained.

Tabel 2

t_{eE} (oC)	Pcd (W)	Pel (W)
-15	175000	97763.49
-10	150000	74065.66
-5	125000	53430.48
0	100000	35906.64
5	75000	21573.15
10	50000	10568.14

Fig. 4 shows an example variant for an intersection between the 2 types of curves mentioned. The intersection point indicates the equality between the necessary power of the consumer and the thermal power delivered by the heat pump, having the abscissa teE. The 3 zones are distinguished: Z1, Z2 and Z3. Zone Z1 corresponds to the thermal power delivered to the power plant consumer, zone Z2 corresponds to the thermal power delivered by the heat pump and zone Z3 corresponds to the thermal power delivered by the heat pump in the conditions of decreasing the electric power used by the car compressor. As can be seen, the mentioned areas are areas of thermal power whose values depend on the outside temperature. Thus for te <teE the heat pump will work with the electric power corresponding to the temperature teE and with a COP corresponding to the respective outdoor temperature, te, and for te> teE the heat pump will work with Pcd = Pnec and with a COP corresponding to the respective outdoor temperature, te. Fig. 5 also shows a qualitative diagram of the thermal and electrical powers in case the equilibrium outdoor temperature is teE = -5 oC. It is observed that in the area of outside temperatures, te, lower than the outside equilibrium temperature, teE, the electric power will be kept constant at the maximum value.

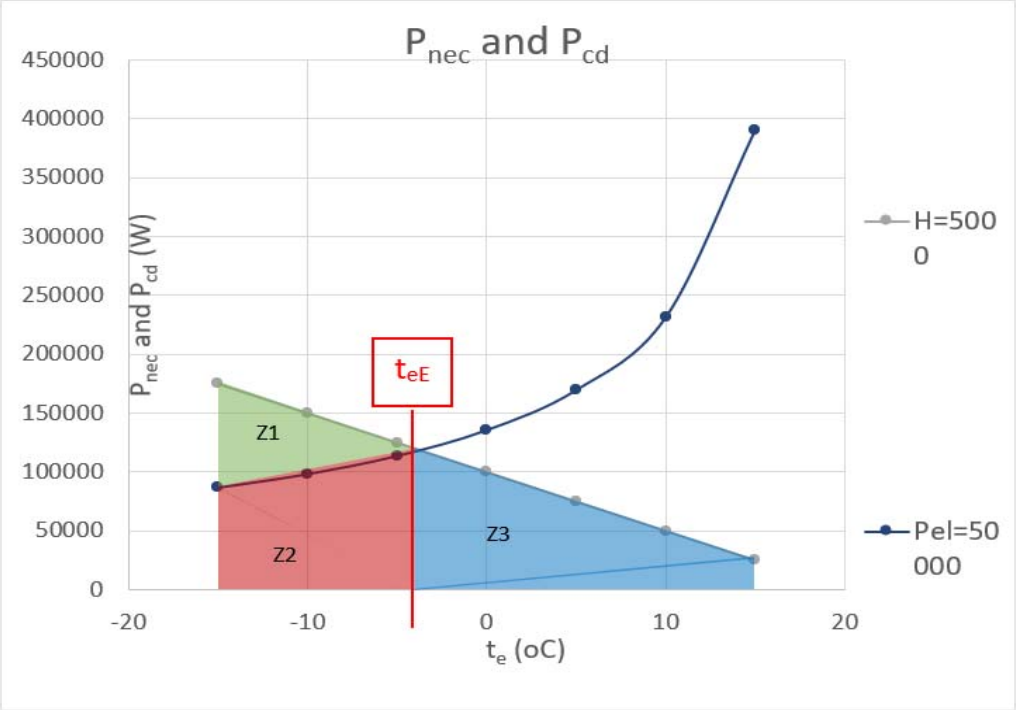

Fig.4

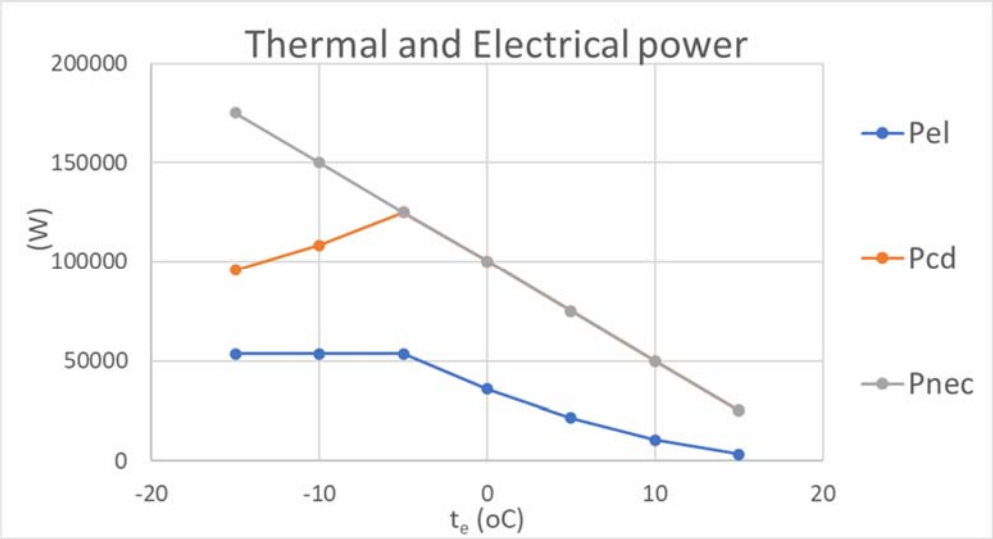

Fig.5

3. Energy considerations

We have a more concrete image in fig.6 which corresponds to a temperature t_{eE} = 0℃. An image like the one in fig.6 is the one presented in fig.7 which now refers to the thermal energies corresponding to these areas. There is a decrease in the share of energy supplied by the boiler while the share of heat supplied by the heat pump has increased. This is due to the frequency of outdoor temperatures that are higher in the range te = -5… 0℃ than in the range t_e = -15… -10℃. Figures 8 and 9 show the diagrams of the electric and thermal powers at the vaporizer and respectively the diagrams of the electrical and thermal energies at the vaporizer.

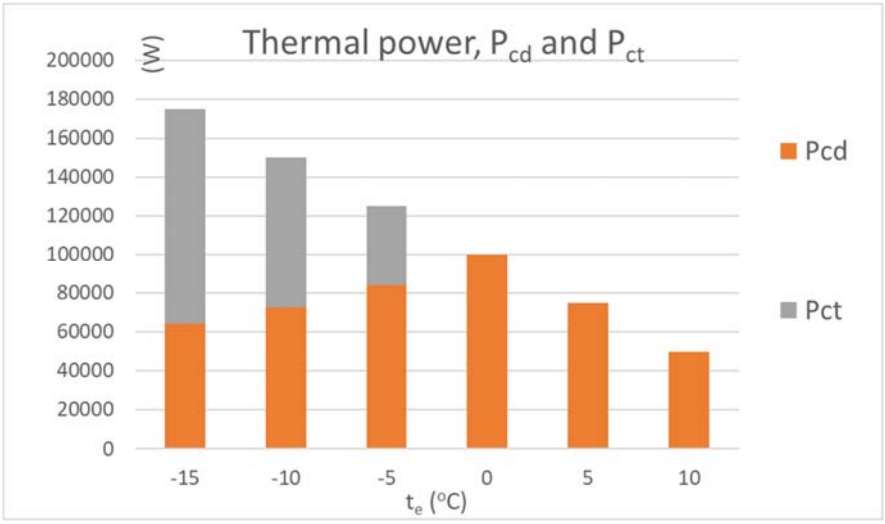

Fig.6

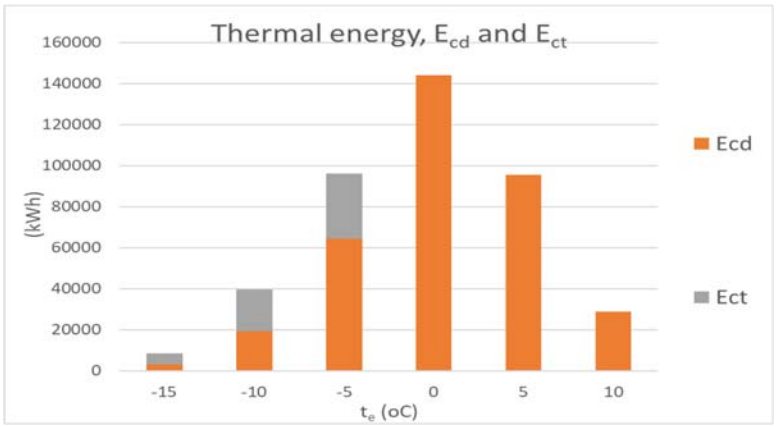

Fig.7

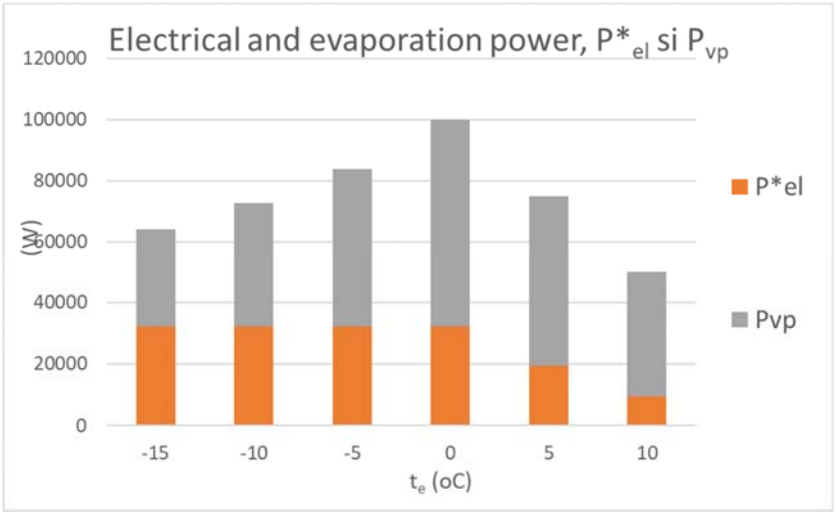

Fig.8

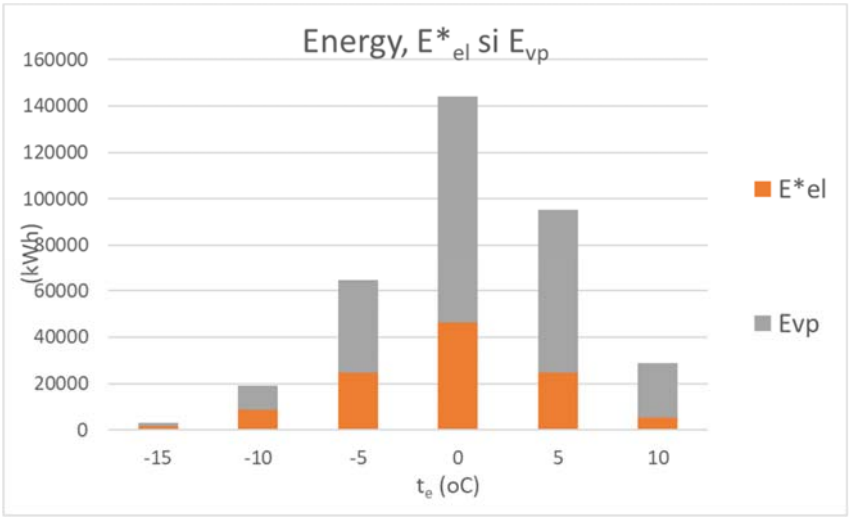

Fig.9

This was done for all variants of sizing the heat pump and finally resulted in the following general situation regarding energy consumption:

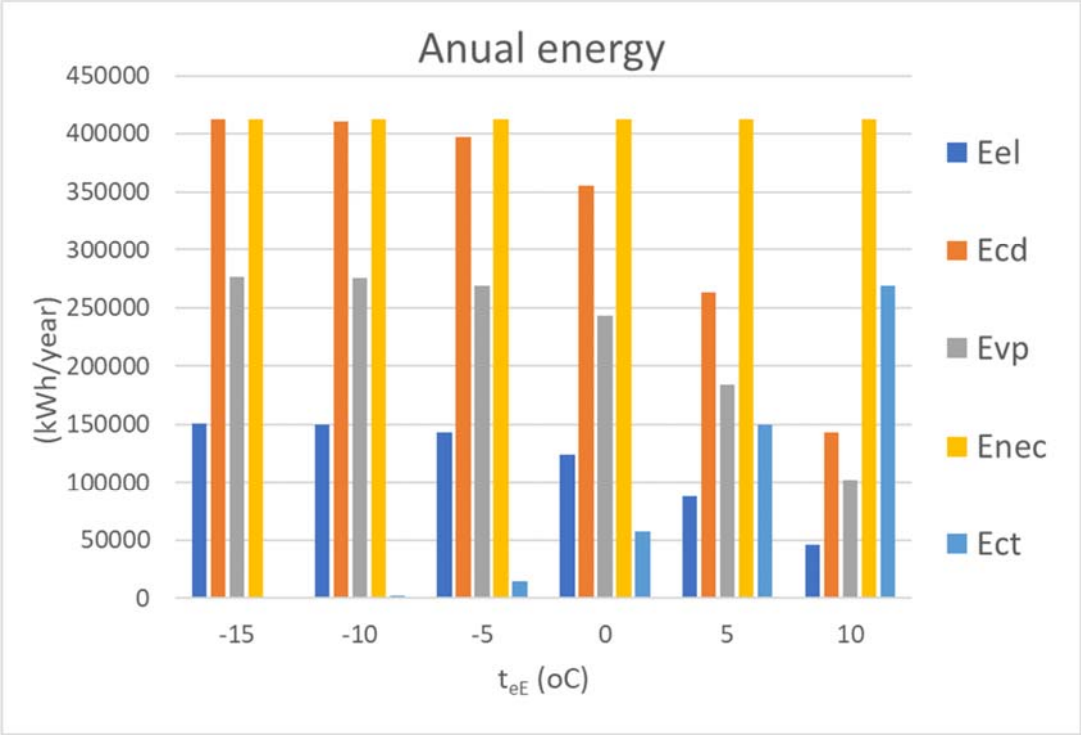

Fig.10

Fig. 10 shows all the categories of energy absorbed and consumed by the source-consumer system. We consider the bar corresponding to the energy absorbed from the environment (renewable) to be acceptable for an external equilibrium temperature, t_{eE}, in the range t_{eE} = -5… 0 ºC. Which means an H / Pel ratio = 0.14 and 0.23.

4. Economic considerations

For the economic evaluation was used Fig.11 which is practically identical to fig.5 in which, however, a series of notations of the important points were made. Thus, the AHCJ trapezoid contains the subsequent thermal diagram necessary for the consumer during the winter. The curvilinear polygon DBCJH contains the diagram of the thermal powers delivered by the heat pump to the consumer, and the curvilinear polygon EFGJH contains the diagram of the electrical powers used by the heat pump. The curvilinear triangle ABD contains the diagram of the thermal powers delivered by the thermal power plant to the consumer. The right segment BI represents the maximum thermal power delivered by the heat pump, and the segments EH and FI represent the maximum electrical power used by the heat pump. The right segment AD represents the maximum power of the thermal power plant. For any equilibrium outside temperature, t_{eE}, results the maximum electric power used by the heat pump and the diagrams of the thermal

powers delivered by the heat pump and by the thermal power plant and the diagram of the electric power used by the heat pump. These diagrams correspond to homologous diagrams by evaluating the associated energies obtained by multiplying the values of the powers with their duration in hours. The costs associated with these thermal and electrical energies are obtained by multiplying the values of the specific costs (lei / kWh_{th} or lei / kWh_{el}).

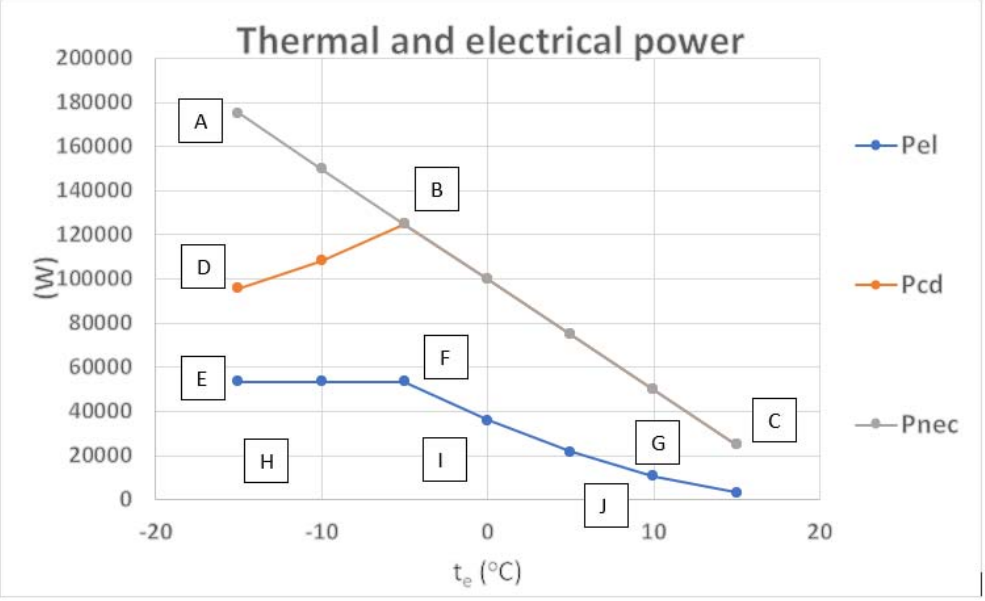

Fig.11

Regarding the investment costs for the heat pump, specific costs were used (lei / Wth or lei / Wel). Thus, for the investment costs, the relations result:

$$CI\_CT = cth\_CT \cdot csi\_CT$$
$$CI\_PC = cth\_PC \cdot csi\_PC \tag{12}$$

And for exploitation costs :

$$CE\_CT = cse\_th \cdot N\_an \cdot \sum_{BIN(-15)}^{BIN(+10)} 24 \cdot Nz_{BIN} \cdot pth\_CT_{BIN}$$
$$CE\_PC = cse\_el \cdot N\_an \cdot \sum_{BIN(-15)}^{BIN(+10)} 24 \cdot Nz_{BIN} \cdot pel\_PC_{BIN} \tag{13}$$

For investment and exploitation costs:

$$CI\_total = CI\_CT + CI\_PC$$
$$CE\_total = CE\_CT + CE\_PC =$$
$$= cse\_th \cdot N\_an \cdot \sum_{BIN(-15)}^{BIN(+10)} 24 \cdot Nz_{BIN} \cdot pth\_CT_{BIN} + \quad (14)$$
$$+ cse\_el \cdot N\_an \cdot \sum_{BIN(-15)}^{BIN(+10)} 24 \cdot Nz_{BIN} \cdot pel\_PC_{BIN}$$

And global cost :

$$C\_total = CI\_total + CE\_total = CI\_total +$$
$$+ cse\_th \cdot N\_an \cdot \sum_{BIN(-15)}^{BIN(+10)} 24 \cdot Nz_{BIN} \cdot pth\_CT_{BIN} +$$
$$+ cse\_el \cdot N\_an \cdot \sum_{BIN(-15)}^{BIN(+10)} 24 \cdot Nz_{BIN} \cdot pel\_PC_{BIN} \quad (15)$$
$$C\_total = CI\_total + CE\_total = CI\_total +$$
$$+ N\_an \cdot \left(\begin{array}{l} cse\_th \cdot \sum_{BIN(-15)}^{BIN(+10)} 24 \cdot Nz_{BIN} \cdot pth\_CT_{BIN} + \\ + cse\_el \cdot \sum_{BIN(-15)}^{BIN(+10)} 24 \cdot Nz_{BIN} \cdot pel\_PC_{BIN} \end{array} \right)$$

From relation (15) it is observed that the graph of the total cost is composed of 2 right segments: a vertical segment at $\tau = 0$ (initial investment) and further a rising line depending on τ (exploitation). And this for each of the variants t_{eE} = -15, -10, -5, 0, +5, +10 ºC. The amounts in the relations (13)… (15) have as units of measurement (kWh / year).

The clear data on which the costs involved over time for various variants of the configuration of the source system were:

Investment specific cost:

Tabel 3

Source type	Specific Cost	(RON/kW)
Heat Pump	csi_PC	1000.0
Centrala Termica	csi_CT	100

Exploitation specific cost :

Tabel 4

Energy type	Specific cost	Var.1 (RON/kWh)	Var.2 (RON/kWh)
Electrical energy	cse_el	0.75	1,401
Thermal energy	csi_th	0.31	0.61

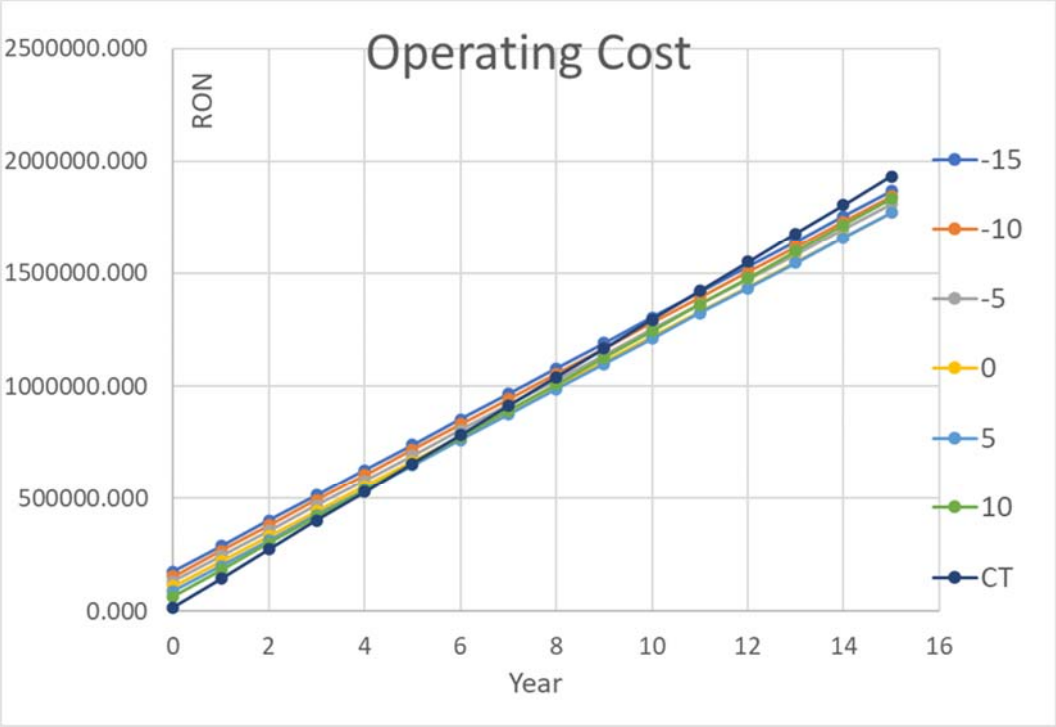

Fig.12

An analysis made on the data presented in fig.12 shows that the recovery times of the investment made for the implementation of a heat pump for serving the space heating consumer depends on the size of the heat pump and therefore on the degree of coverage offered by it. Thus, the results presented in fig.13 were obtained:

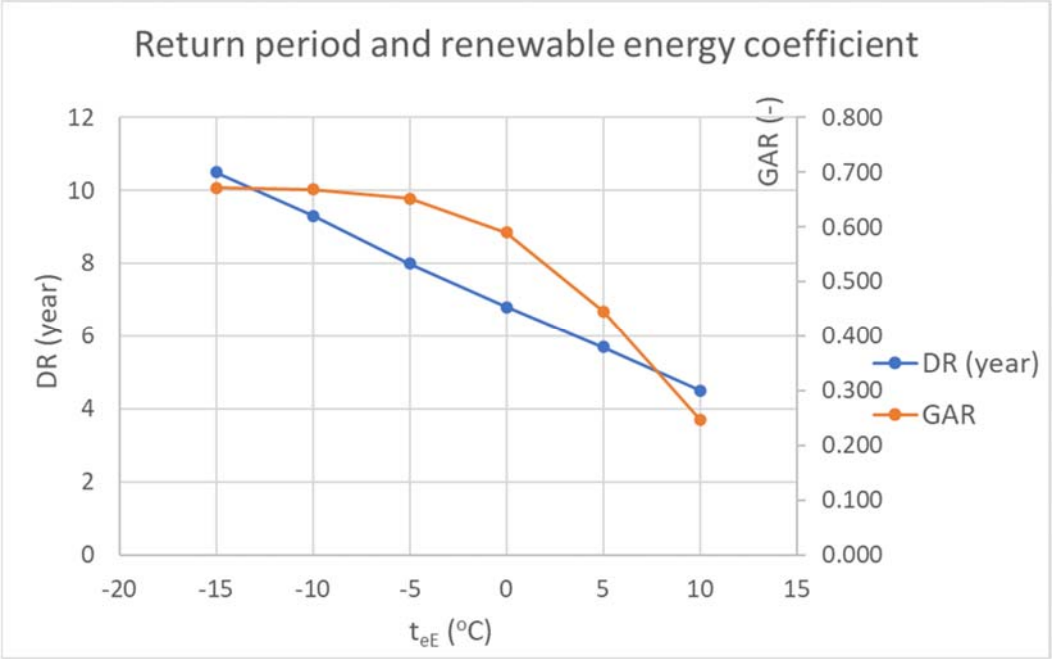

Fig.13

As we believe it to be, a lower equilibrium outside temperature, teE, means a higher heat pump. According to the results presented in fig. 13 we opt for a choice of heat pump so that it allows a coverage of energy consumption of approx. 60% - 65% of the maximum possible of approx. 70%. This results in a recovery of the investment of cc, 7-8 years.

5. Conclusions

The simplified procedure presented in this paper is based on the detailed procedure presented in previous papers [1]… [4], the novelty aspect being the dependence of the COP of the heat pump on the difference between the temperatures of hot and cold environments. θ_{CD} and θ_{VP}. The simplification consists in giving up the iterative process of determining the COP for the situations in which the result is a slight underestimation of the value of the COP. The relation (2) that expresses the dependence of the Carnot refrigeration efficiency on the temperature difference $\Delta\theta$, we can say that it is specific to the case in which the consumer is a central heating installation, in another situation, for example the preparation of hot water. more appropriate correlation. 15 The use of heat pump for space heating leads to the conclusion that the choice the capacity of the heat pump compared to the capacity of the consumer heating system must be made so that the equilibrium outside temperature, teE, is situated in the range te = [-5… 0) °C, which corresponds to values of the H / Pel ratio = 0.14… 0.23, which means that the heat pump must cover the heat demand of to the consumer at an outside temperature in the range te = (-5… 0) °C. This is is mainly due to the fact that the frequency of outdoor

temperatures is most according to the outside temperature te> -5 °C. In other words, the optimal ratio between the capacity of the heat pump and the capacity of the heating system should be included in the range 0.57 and 0.71.

ANEXA

We consider it useful to present in this ANNEX the simple procedure by which the isentropic yield can be determined, ηIZ, when a series of information regarding the catalog values for COP0, θVP0, θCD0, PCD0, ηEL is available. This simple procedure was also presented in [4].

- Establishes the catalog power that can be absorbed from the grid:

$$P_{EL0} = \frac{P_{CD0}}{COP_0} \tag{A.1}$$

Catalog CARNOT refrigeration efficiency is established, εCVP0 and catalog isentropic refrigeration efficiency:

$$\varepsilon_{VP0}^{C} = \frac{\theta_{VP0} - \Delta t_{VP} + 273.15}{\theta_{CD0} - \theta_{VP0} + \Delta t_{CD} + \Delta t_{VP}}$$
$$\varepsilon_{VP0}^{IZ} = M \cdot \varepsilon_{VP0}^{C} - N \tag{A.2}$$

1. Establish the isentropic efficiency of the compressor:

$$\eta_{IZ} = \frac{COP_0 - \eta_{EL}}{\varepsilon_{VP0}^{IZ} \cdot \eta_{EL}} \tag{A.3}$$

Nomenclature:

t_{i0} – interior design temperature, °C;
t_{e0} – exterior design temperature, °C;
t_{T0} – design turn thermal agent temperature, °C;
t_{R0} – design return thermal agent temperature, °C;
t_{m0} – design average temperature, °C;
t_e – external temperature, °C;
t_{eE} – equilibrium external temperature, °C;
T_{VP} – absolute vaporization temperature, K;
T_{CD} – absolute condensing temperature, K;
Δt_{VP} – vaporization temperature difference, °C;
Δt_{CD} – condensing temperature difference, °C;

θ_{VP} – cold environment temperature, ^oC;
θ_{VP0} – design cold environment temperature, ^oC;
θ_{CD} – hot environment temperature, ^oC;
θ_{CD0} – design hot environment temperature, ^oC;
P_{VP} – vaporization heat, W;
P_{CD} – condensing heat, W;
P_{CD0} – design condensing heat, W;
P_{nec} – heat demand, W;
P_{EL} – electrical power of compressor motor, W;
P_{EL0} – maximum electrical power of compressor motor, W;
P_{CT} –boiler power, W;
E_{VP} – evaporation energy, kWh;
E_{CD} – condensing energy, kWh;
E_{EL} – electrical energy absorbed, kWh;
E_{nec} – demand thermal energy, kWh;
E_{CT} – thermal energy from boiler, kWh;
H – building global thermal coefficient, W/K;
ε^C_{VP} – heat pump Carnot efficiency, -;
ε^C_{VP0} – design heat pump Carnot efficiency, -;
ε^{IZ}_{VP} – vaporization isentropic efficiency, -;
ε^{IZ}_{VP0} – design vaporization isentropic efficiency, -;
COP – coefficient of performance, -;
COP_0 – design coefficient of performance, -;
η_{iz} – isentropic compressor efficiency, -;
η_{EL} – compressor motor electrical efficiency, -;
M = 0.958, N = 1.5321 – isentropic efficiency regression coefficients, -
csi_CT – specific investment cost, boiler, lei/kW;
csi_PC – specific investment cost, heat-pump, lei/kW;
cse_th – thermal energy specific cost, lei/kWh;
cse_el – electrical energy specific cost, lei/kWh;
cth_CT – boiler thermal capacity, kW;
cth_PC – heat pump thermal capacity, kW;
pel_PC – heat pump absorbed electrical energy, kW;
pth_CT – delivered boiler heat, kW;
Nz_{BIN} – BIN days, day;
N_an – operating years of hybrid system, year;
CI_CT – investment cost for boiler, RON;
CI_PC – heat pump investment cost, RON;
CE_CT – yearly operating cost for boiler, RON;
CE_PC – yearly operating cost for heat pump, RON;

CI_total – total investment cost, RON;
CE_total – total operating cost, RON;
C_total – total cost, RON;

References

[1] – Florin Iordache, Alexandru Draghici – Procedura de evaluare a indicatorilor de performanta pentru masini frogorifice sau pompe de caldura – Revista Romana de Inginerie Civila, volumul 10 (2019) nr.4 - editura Matrixrom, Bucuresti;

[2] – Florin Iordache, Alexandru Draghici, Mugurel Talpiga – Comportamentul termic dynamic al unei pompe de caldura functionand intre 2 rezervoare de acumulare – Revista Romana de Inginerie Civila – volumul 10 (2019) nr.4 – editura Matrixrom, Bucuresti;

[3] – Florin Iordache, Mugurel Talpiga – Aspecte privind optimizarea constructiv functionala a unui sistem de pompa de caldura cu compresie (cu sursa de rezerva) pentru incalzirea unei cladirirezidentiale sau prepararea apei calde de consum – Revista Romana de Inginerie Civila, volumul 10 (2019) nr.2 – editura Matrixrom, Bucuresti;

[4] – Florin Iordache, Mugurel Talpiga, Alexandru Draghici - Hibrid system energetic performance evaluation composed by vapor compression heat pump used in building heating and dailly hot water – Revista Romana de Inginerie Civila, volumul 13 (2022) nr.2 – editura Matrixrom, Bucuresti;

Influența generatoarelelor sincrone cu magneți permanenți în industria energiei regenerabile

The influence of permanent magnet synchronous generators in the renewable energy industry

Emilia Dobrin[1]

[1]Timișoara Polytechnic University
Victoria Square 2, Timișoara 300006, Romania
E-mail: emi_dobrin@yahoo.com

Rezumat: *Generatoarele sincrone cu magneți permanenți sunt esențiale în buna funcționare a lanțului de conversie a energiei regenerabile – eoliene, de aceea sunt subliniate tipurile de geometrii constructive ale rotoarelor acestora. Lucrarea de față este un studiu bibliografic care vine în sprijinul producătorilor de top ai centralelor eoliene, pentru a ușura munca acestora de proiectare. Un rol important al GSMP este dat de magneți permanenți din pământuri rare care asigură o cantitate ridicată de energie magnetică necesară funcționari excelente a GSMP, ceea ce ii recomandă producătorilor de centrale eoliene.*

Cuvinte cheie: GSMP, magneti permanenti din pamanturi rare, conversie energetică.

Abstract: *Synchronous generators with permanent magnets are essential in the good functioning of the renewable energy - wind energy conversion chain that is why the types of constructive geometries of their rotors are highlighted. The present work is a bibliographic study that supports the top manufacturers of wind power plants, in order to facilitate their design work. An important role of the SGPM is given by permanent magnets from rare earths that provide a high amount of magnetic energy required for excellent functions of the SGPM, which is recommended for wind power plant manufacturers.*

Keywords: SGPM, rare earth permanent magnets, energy conversion.

DOI: 10.37789/rjce.2022.13.4.4

1) Introduction:

The first commercial appearance of the synchronous generator can be dated to August 24, 1891, with the demonstration that was carried out at an international electrical exhibition Lauffen in Frankfurt, this demonstration was so convincing regarding the feasibility of transmitting a.c. power, over long distances, that the city of Frankfurt adopted it for their first power plant, commissioned in 1894 [1]. Since then and until now, synchronous generators have changed many constructive geometries

until they have the constructive forms we know today. In the last decade, permanent magnet synchronous generators have become increasingly prevalent in industrial applications: GSMPs are widely used in: renewable energy systems - especially in new generations of wind power plants, servo - industrial applications due to their high performance characteristics, space, automobiles, electronics, exploitation and research equipment [2].

2) Structural elements. The principle of operation

The synchronous electric generator belongs to the family of electric rotary machines. The electric generator, polyphase alternating current, usually three-phase, of each rotor tends to align with the rotating field produced by the stator, their rotor has an angular speed equal to the synchronism speed Ω (the angular speed of the rotating magnetic field). The magnetization of the rotor is produced by the permanent magnets in the rotor. This type of generator is called a synchronous generator (SGPM) and is shown in figure 1. Or simply put, it is a synchronous machine where the classic excitation winding is replaced by a permanent magnet, thus becoming electric machines without a brush-ring system [3].

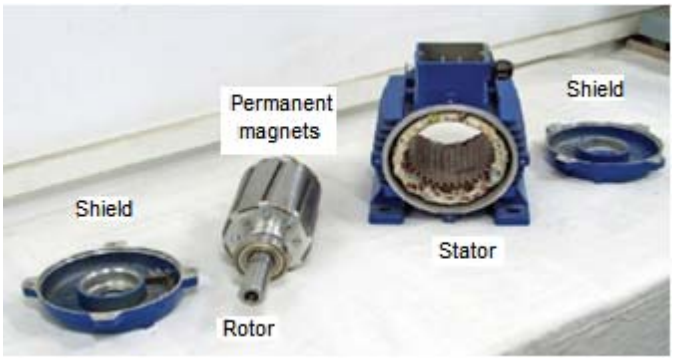

Fig. 1 The component elements of a SGPM [4]

The rotor presents a great constructive diversity, from which the variants can be distinguished:

- according to the construction method we have:

a) **The rotor with apparent poles** has the magnetic circuit made of sheet metal or solid steel with the coils of the excitation rotor winding in series and arranged on these poles. This construction is simpler and cheaper, but presents reduced mechanical safety at high speeds.

b) **The rotor with submerged or smooth poles** has a cylindrical magnetic circuit. It is executed as a package of sheets or solid steel with high mechanical resistance. The rotor winding, called the excitation, made up of series coils, is placed in slots made on the generators on the outside of the rotor. Slots are not evenly distributed on the rotor circumference, each pole corresponds to a polar "tooth" (the space between two slots) called "wide tooth", shown in figure 2.

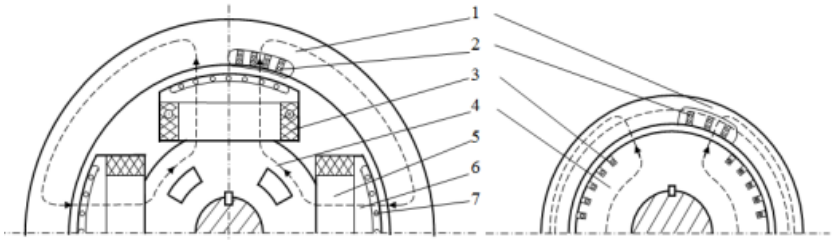

a) b)

Fig. 2 Basic constructive elements of synchronous generators: a) with apparent poles; b) with submerged poles. 1-stator yoke, 2-stator winding (induced), 3-rotor winding (inductor), 4-rotor yoke, 5-rotor pole, 6-pole piece, 7-damping winding [5].

The rotor can be made with permanent magnets in which case there are solutions:
c) **Radial flow rotor** are the most conventional rotors for SGPM as can be seen in figure 3. We obtain a higher power due to the increase in machine length and a flexibility for high scaling. It is mainly used in: wind systems, traction, ship propulsion, robotics [6].

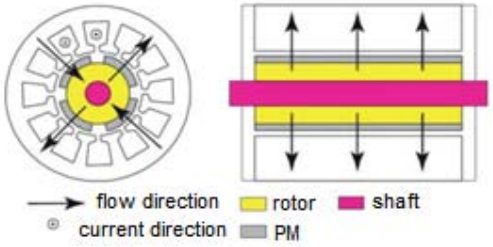

Fig. 3 Cross-sectional view in the radial direction and in the axial direction, respectively, of a typical SGPM radial flow [6]

d) **In axial flow machines**, the length of the machine is much reduced compared to radial flow machines, shown in figure 4. Their main advantage is high torque density, so they are recommended for applications with size restrictions, especially on axial direction [6]. One of the disadvantages of axial flow machines is that they are not balanced in the single rotor and stator edition. Usually, for better performance, the rotor is sandwiched between two stators or vice versa.

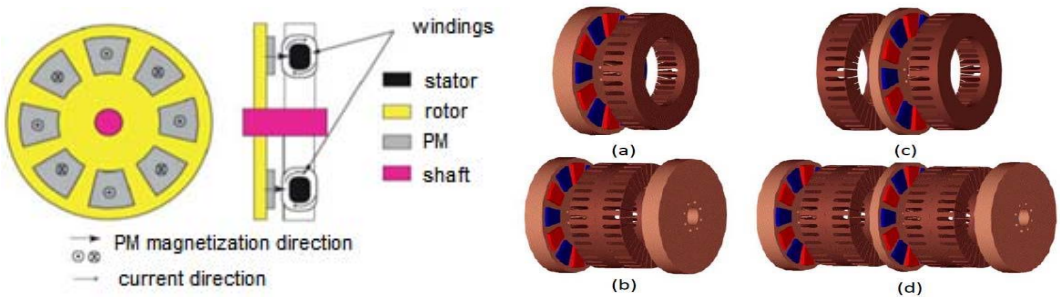

Fig. 4 Cross-sectional view in the radial direction and in the axial direction, respectively of a typical SGPM axial flow [6, 7].

e) **In cross-flow machines**, the plane of the flow path is perpendicular to the direction of rotor movement. The use of cross-flow machines can be proposed in applications with a high level of torque density. An attractive property of transverse flux machines is that the current loading and magnetic loading can be adjusted independently. Figure 5 shows a fraction of a typical SGMP crossflow.

A disadvantage of transverse SGMP is high leakage flux leading to poor power factor. Another disadvantage is that in turning the SGMP transversely, the mechanical construction is weak due to the large number of parts. They are used in: wind systems, free piston generators for hybrid vehicles, the ship's propulsion and wind system, applications with high torque density [6].

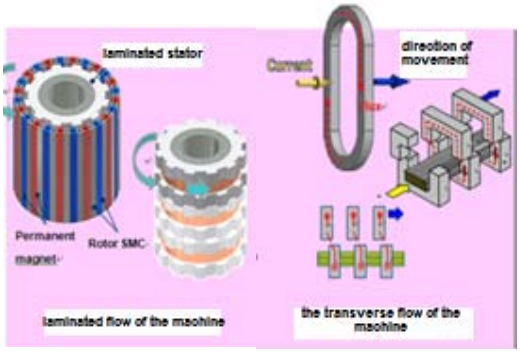

Fig.5. Representation of transversal flows [6]

f) The rotor surrounds the stator in **external rotor** machines. In these machines, the magnets are usually located on the inner circumference of the rotor. Consequently, for the same outer diameter of the machine, in the outer rotor machine the rotor has a larger radius compared to the stator and it can be equipped with a larger number of poles for the same pitch. Another advantage is that the magnets are well supported despite the centrifugal force. In addition, better cooling of the magnets is provided. Outboard rotor machines are common for small HAWT turbines, where sometimes the hub carrying the blades is directly attached to the rotor.

g) However, **inner rotor** machines are a more common solution on the market today. In small machines the main contributors to losses are copper losses and therefore the stator winding has the largest temperature rise in the active material of the machine. Figure 6 shows a SGPM inner rotor and a SGPM outer rotor [6].

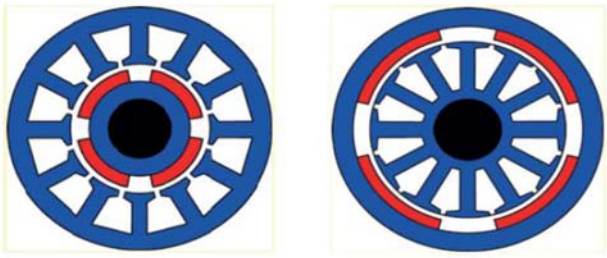

Fig.6. SGPM inner rotor (left) and SGPM outer rotor (right) [6].

From the point of view of the configuration of the permanent magnets, they can be mounted:

h) Surface mounted magnets

A common topology is where the magnets are mounted on the surface of the rotor, sometimes referred to as the **outer magnet**. Magnets are glued and/or "bandaged" to the inner surface of the rotor to resist the centrifugal force, as can be seen in figure 7. Usually, the magnets are oriented or magnetized in the radial direction and less often in the circumferential direction. The direction and quadrature of the reactances are almost equal. The construction of the rotor core in the SGPM is the easiest of the PM configurations due to the simple geometry of the rotor. Here the PMs are radially magnetized.

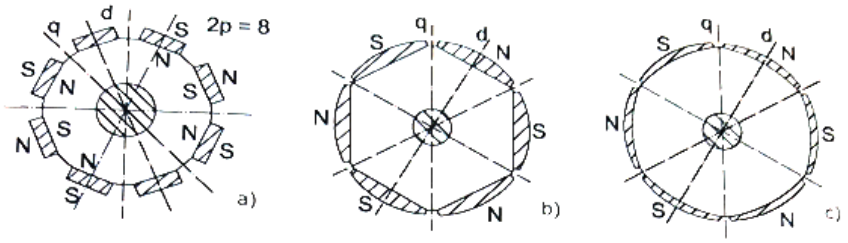

Fig. 7 Features SGPM rotor surface mounted magnets [7]:
a) uniform thickness surface magnet
b) type magnet “bread leaf”
c) deconcentrated magnets

By placing them outside the rotor directly in the air-gap, there is a corresponding reduction of the mass and therefore of the moment of inertia [7].

i) Inserted magnets

In machines with **inserted magnets**, the rotor core of the machine is modified with iron interpoles, represented in figure 8. Iron interpoles are prominent of the rotor core wherever magnets are not present on the surface. Interpoles cause silence and inductances give different straight and quadrature directions. In these machines, part of the torque is reluctance torque and the torque density is higher compared to SGPM. The magnets are radially magnetized. Flux leakage is higher compared to SGPM, resulting in lower power factor. Therefore, in direct drive application, inverter usage is less as compared to geared applications. This topology is not common in gearless wind systems [6].

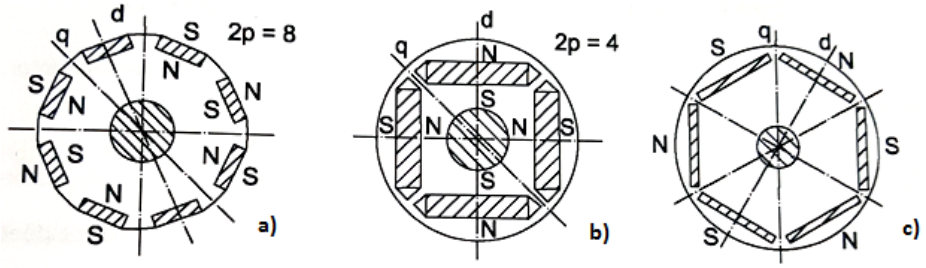

Fig.8 Features built-in magnets for SGPM rotor [7]:
a) medallion type magnets; b), c) internal magnets with a single layer.

j) **Disc type magnets**

MP from rare earths characterized by high coercive magnetic field values are used. The rotor has the shape of a disc. Permanent magnets are axially magnetized and are shown in figure 9. They are mainly used in wind power plants [8].

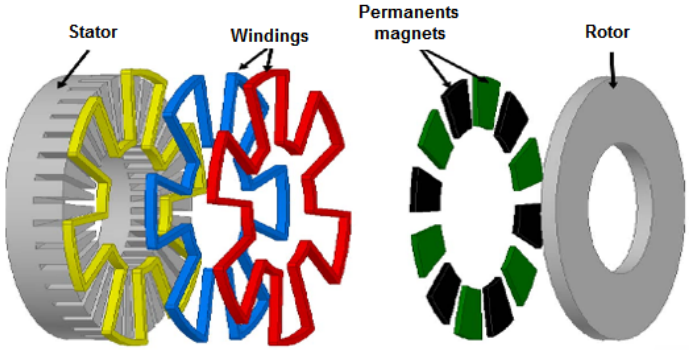

Fig. 9 Represents disc type magnets [9]

Another classification of SGPM is made according to the type of winding:
Windings can be divided into overlapping and non-overlapping categories. Non-overlapping windings can only be wound in concentrated mode. The overlap term is usually omitted. For example "overlapping winding" is almost always referred to as distributed winding. In this text, on the other hand, "concentrated winding" means "concentrated winding that does not overlap with two layers", as in figure 10 [6].

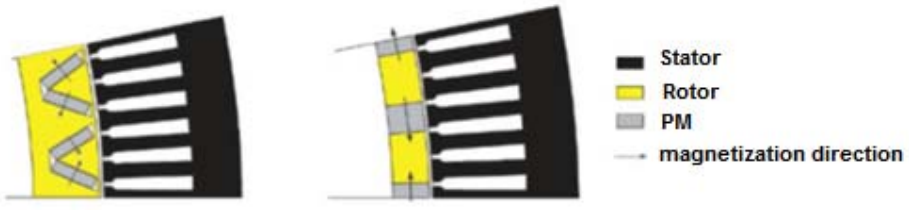

Fig.10 Cross section of a pair of poles of a V-shaped buried magnet design (left) and a tangentially buried magnet design (right) [6]

3) Permanent magnets used for SGPM

The use of permanent magnets with high stored energy density as motor excitation sources leads to high performance SGPM s in terms of high power density, net superior efficiency and reliability, and high speed [10].
In the following we present comparatively the four classes of magnets used in the construction of generators [11,12]:

Classes of magnets *Tabel 1*

AlNiCo	FERRITE	SmCo	NdFeB
They can be isotropic and anisotropic	Breakable	They are high energy PMs	They are the strongest on the market
It is obtained by casting and sintering	It is obtained by sintering	It is obtained by sintering	It is obtained by sintering
Low coercive field (160[kA/m])	High coercive field (265[kA/m])	Very high coercive field (700[kA/m])	Highest coercive field (1000[kA/m])
High remanent induction (1.35[T])	Low remanent induction (0.39[T])	Medium remanent induction (1.05[T])	High remanent induction (1.35[T])
Low magnetic energy	Low magnetic energy	High maximun magnetic energy	High maximum magnetic energy
Good corrosion resistance	Good corrosion resistance	High corrosion resistance	Fragile
High termic resistence	High termic resistence	Stabile termic resistence	Moderate termic resistence
-	Maximum work temperature 400^0C	-	Low work temperature 150^0C

Data are compiled from technical sheets of different PM manufacturers (for the year 2019), for temperatures between 20 - 30◦C. Hci is the intrinsic coercivity of the MP, for alnico MP the normal coercivity is given (since the data sheets do not give Hci). No *CBmin* MP is given for alnico because that material class is typically used on a minor degaussing loop and *Cbmin* MP therefore depends on which minor loop is chosen. When μrec is not given, it is estimated by μrec = B^2r/(4μ0|BH|max), i.e. assuming the maximum energy occurs in the linear part of the magnetization curve, the estimated μrec are marked with a "*". Worldwide it is noted that the demand for permanent magnets is increasing, especially for those made of neodymium [13].

Properties of MP materials available on the market [13] *Tabel 2*

Magnet type	Br [T]	Hci [kA/m]	|BH|max [kJ/m3]	Mrec [-]	CBminMP [-]
Alnico	0.55–1.37	38–151	10.7–83.6	1.3–6.2	-
Hard ferrite	0.20–0.46	140–405	6.4–41.8	1.05–1.2	−0.4–0.4
Nd-Fe-B	1.08–1.49	876–2710	220–430	1.0–1.1 *	−2.3–0.2
Sm-Co	0.87–1.19	1350–2400	143–251	1.0–1.1 *	−2.7−0.62

Figure 3.1 shows the market demand for permanent magnets from rare earths with 59%, followed closely by those from ferrites with 31%.

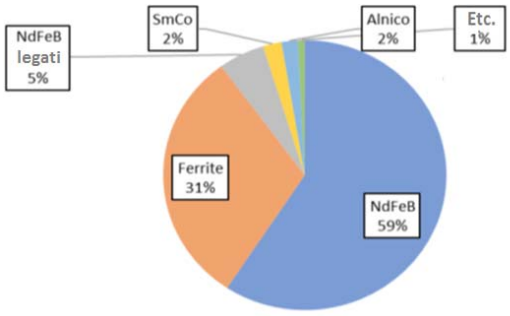

Fig.3.1 Current share of MP demand worldwide [14]

The estimate of the market of permanent magnets relative to the price per kilogram is presented in table 3. Permanent magnets from rare earths - NdFeB have the highest price [15].

It represents the price/kg value of PM [15] *Tabel 3*

MATERIAL [-]	COST [$]/PERFORMANTS [-]	MASS[tone]
NdFeB	11,200	160,000
Ferrite	5,800	830,000
SmCo	400	4,200
AlNiCo	350	6,300

For wind power plants, development is currently in the direction of permanent magnet generators. These advantages have led to the current situation where synchronous generators produce over 90% of the electricity in Romania, but also in the world.
The advantages of opting for such a SGPM: they have the highest efficiency (over 90%), they are the only ones that provide both active and reactive energy, they allow the frequency and voltage to be kept constant, low operating noise, reliability, high efficiency.
Disadvantages of SGPM: increased cost price, safety, demagnetization of magnets, ability to operate at high speed.

4) Mathematic Model of the Synchronous Generator

Mathematical modeling of SGPM is an essential condition to be able to obtain generator control algorithms, as well as dynamic characteristics for wind energy conversion systems [16]. For the mathematical model of the SGPM in dq0 or the orthogonal model represented in figure 4, the rotating frame of reference will also be extended to the SGPM torque analysis. The tension function of the SGPM in reference to the dq axes of the frame can be expressed as follows [17, 18].

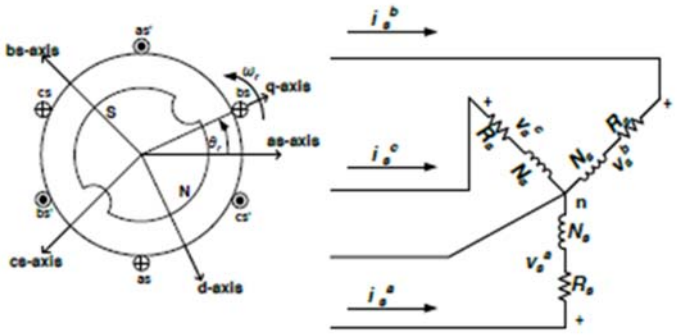

Fig. 4 Orthogonal model [19]

$$U_d = R_a i_d + L_d \frac{di_d}{dt} - \omega L_q i_q \quad (1)$$

$$U_q = R_a i_q + L_q \frac{di_q}{dt} + \omega L_d i_d + \omega\varphi \ (2)$$

$$\omega = p\Omega \ (3)$$

Where:

Vd, Vq, id, iq – dq0 components of stator voltage and current;
Ra – resistence of stator winding;
Ld, Lq – stator winding inductance;
φ – permanent magnetic flux;
p – pole pairs number;
Ω – magnetic flux;
ω = generator electrical angular speed;
The equation of electromagnetic torque has this expresion:

$$T_{em} = \frac{3}{2} p \left(L_d - L_q\right) i_d i_q + \varphi i_q) \ (4)$$

The voltage equations of the stator circuit are given by (7), where x ∈ {a, b, c}.

$$v_s^x = R_s i_s^x + \frac{d}{dt} \lambda_s^x \ (5)$$

The SGPM has sooth poles (Ld = Lq = Ls), replacing the formula of voltage in the current one [18]:

$$\frac{dt_d}{dt} = -\frac{R_a}{L_s} i_d + \omega i_q + \frac{1}{L_s} U_d \ (6)$$

$$\frac{dt_q}{dt} = -\frac{R_a}{L_s} i_q - \omega \left(i_d + \frac{1}{L_s}\varphi\right) + \frac{1}{L_s} U_q \ (7)$$

The generator was modeled considering the scheme shown in the figure below 3. The voltage function of the SGPM in the *dq* - axes reference frame can be expressed as follows [13] and [14].

5. Conclusions:

The permanent magnet synchronous generator is one of the most attractive generators for wind power plants. This type of generator can work for any size wind farm from kW (or even several hundreds of watts) to many MW.

By choosing to use SGPM we have a number of advantages:

1. High efficiency: SGPM are the highest efficiency class of electric machines. This is due to the existence in their structure of permanent magnets as a source of excitation and which do not require energy consumption from outside the machine. The absence of the mechanical switch and the ring-brush system reduces mechanical friction, implicitly mechanical losses, which adds an extra to the efficiency.

2. Compaction: The relatively recent appearance of high energy density permanent magnets (rare earth magnets) allow high flux densities to be achieved in SGPM. That leads to obtaining high torque density, so implicitly, it reduces the dimensions and weight of the machine.

3. Simplicity in control: SGPM can be controlled very simply, invoking strategies and methods very well developed at the moment.

4. Simplicity in cooling: since there is no electric current circulation in the rotor, it does not heat up, so it does not need cooling. The stator of the machine is the one through which the electric current passes, and its need for cooling is satisfied at the level of the outer periphery of the machine casing.

5. Simple maintenance, pronounced longevity and high reliability: The absence of brushes and mechanical switch suppresses the need for periodic maintenance and the risk of failure of these components.

6. Very low noise emissions: Not being a mechanical switch but an electronic one, the machine is very quiet, and if the electronic control converter is operated at high frequencies, the noise produced by the switch goes beyond the perceptible zone of the human ear.

Bibliography

[1] ***NTHU, Principles of operation of synchrous machines, Ed.Wiley J.and sons;
[2] *J., Gieras,* Permanent Magnet Motor Technology: design and applications, 3rd edition, Ed. Taylor & Francis CRC Press Group, 2014;
[3] *E., Erina,* Optimizarea proiectării unui generator sincron ce echipează o microhidrocentrală, Teza doctorat, 2012;
[4] ***MARKETWATCH - O nouă marca ICPECA mașini electrice, articol;
[5]***ETH.IEEIA.TUIASI – Mașina sincronă, Considerații generale, Curs de laborator;
[6] *R., Kumar*, Study of permanent magnet synchronous generator, Dissertation Thesis of, 2015;
[7] *N., Stirban,* Low cogging torque PMSM drives with rectangular current control, Phd. Thesis, 2010;
[8] *S., Muşuroi,* Acţionări electrice cu servomotoare, Ed. Politehnica, Timişoara, 2006;
[9] *A., Multi, I., Garniwa*, Relationships between excitation voltages and performance of AFWR synchronous generator, www.researchgate.net, 2013;
[10] *E., Furlani*, Permanent Magnet and Electromechanical Devices, Elsevier;
[11] ***EUROMAGNET – Magnet neodim, supermagnet permanent;
[12] *S., Muşuroi*, Acţionări electrice cu servomotoare, Ed. Politehnica, Timişoara, 2006;

[13] *P., Eklund, S., Eriksson,* The influence of permanent magnet material properties on generator rotor design, ed. Energies, 2019;
[14] *J., Ormerod,* Technology Advisor Magnet Applications, Magnet Applications, Inc.DuBois, Pennsylvania, USA;
[15] ***SLIDESHARE - J., Ormerod, Rare Earth Magnets: Yesterday, Today and Tomorrow, 2019;
[16] M., HANNACHI, M., BENHAMED Modeling and Control of a Variable Speed Wind Turbine with a Permanent Magnet synchronous Generator, 2017 International conference on green energy conversion systems (GECS), pp.1–6. IEEE, 2017;
[17] *J. S., Thongam, P., A. Bouchard,* Control of variable speed wind energy conversion system using a wind speed sensorless optimum speed MPPT control method, In IECON 2011-37th Annual Conference on IEEE Industrial Electronics Society (pp. 855-860), 2011;
[18] *H., Geng, D., Xu,* Stability analysis and improvements for variable-speed multipole permanent magnet synchronous generator based wind energy conversion system, IEEE Transactions on Sustainable Energy, *2*(4), 459-467, 2011;
[19] *P., Krause, O., Wasynczuk*, "Analysis of Electric Machinery and Drive Systems", Third Edition, IEEE PRESS 2013, Wiley.

Cheap building material prepared by unconventional heating of glass waste in alkaline solution

Material de construcție ieftin fabricat prin încălzirea neconvențională a deșeului de sticlă în soluție alcalină

Lucian Păunescu[1], Sorin-Mircea Axinte[2,3]

[1] Cosfel Actual SRL
95-97 Calea Grivitei street, M4 room, sector 1, Bucharest 010705, Romania
E-mail: lucianpaunescu16@gmail.com

[2] Daily Sourcing & Research SRL
95-97 Calea Grivitei street, sector 1, Bucharest 010705, Romania
E-mail: sorinaxinte@yahoo.com

[3] Department of Applied Chemistry and Material Science, University „Politehnica" of Bucharest
1-7 Gh. Polizu street, sector 1, Bucharest 011061, Romania
E-mail: sorinaxinte@yahoo.com

DOI: 10.37789/rjce.2022.13.4.5

Rezumat. *Spumă de sticlă fabricată din deșeu de sticlă și soluție apoasă de silicat de sodiu (apă de sticlă) cu excelente proprietăți termoizolante (densitate între 0,25-0,33 g cm^{-3}, conductivitate termică între 0,059-0,069 W $(mK)^{-1}$, porozitate între 84,3-88,1 %) pentru aplicații în construcții a fost realizată cu succes folosind o tehnică originală de încălzire cu microunde predominant directă aplicată de autori, spre deosebire de metodele convenționale utilizate în mod obișnuit la fabricarea spumei de sticlă. Lucrarea a testat utilizarea apei de sticlă ca agent de spumare în condițiile particulare ale încălzirii cu microunde, deși capacitatea sa este cunoscută doar ca material de anvelopare în procesele de spumare cu agent carbonic lichid.*

Cuvinte cheie: spumă de sticlă, încălzire cu microunde, apă de sticlă, soluție apoasă alcalină.

Abstract. *Glass foam made of glass waste and aqueous sodium silicate solution (water glass) with excellent thermal insulation properties (density between 0.25-0.33 g cm^{-3}, heat conductivity between 0.059-0.069 W $(mK)^{-1}$, porosity between 84.3 -88.1 %) for building application was successfully performed using an original predominantly direct microwave heating technique applied by the authors, unlike the conventional methods commonly used in glass foam manufacturing. The paper tested the use of water glass as a foaming agent under the particular conditions of microwave heating, although its ability is known only as an enveloping material in foaming processes with liquid carbonaceous agent.*

Key words: glass foam, microwave heating, water glass, aqueous alkaline solution, thermal insulation properties.

1. Introduction

Glass foam remakably combines a multitude of properties (light weight, physical rigidity, resistant to fire, water, and steam, chemically inert, non-toxic, thermally insulator, frost resistant, resistant to rodent, insect, bacteria, resistant to compression, etc.) which make it attractive for several fields of application, primarily in construction. Initially (in the 1930s), the basic raw material was finely ground pure glass mixed with a gas-supplying material under high temperature conditions (most often carbon or carbonaceous materials). The heat treatment of mixture creates the conditions for the release and spread of gases in the thermally softened mass of the glass forming numerous bubbles, which by the final cooling turn into pores. Such a heat-insulating and non-flammable structure to glass foam was used by the United States during World War II for the inner lining of ships and submarines [1].

The onset of the world energy crisis and the perception of the danger of global overheating due to the uncontrolled emission of greenhouse gases in the last decades of the 20th century have significantly changed the attitude of humanity towards the huge reserve of waste accumulation worldwide.

One of the important quantitative wastes with very high annual generation rates is glass waste maintly from post-consumer drinking bottles as well as from the demolition or redevelopment of buildings in the form of flat glass (around 130 million tons, of which 48 % are container glass and 42 % flat glass) [2]. Recycling this waste is currently aimed at ensuring the basic raw material of industrial processes for the manufacture of glass foam. Numerous facilities have developed in recent decades in several European countries, the United States, and China, which industrially produce various types of glass foam using recycled glass waste as the main raw material. The most important companies that dominate the glass foam market are Misapor (Switzerland), Pittsburgh Corning (USA), Geocell (Austria), and Glapor (Germany) with branches in different countries [3]. The manufacturing recipes of each glass foam producer differ mainly by the nature of expanding agents, the most commonly used being black carbon, calcium carbonate, glycerine, and silicon carbide [1] in association with various mineral additives that favor the glass expansion process.

Small-scale laboratory science conducted in the last 20-25 years worldwide aims to further investigate the manufacturing feasibility of many other types of glass foam using various assortments of glass waste [4-7] and other silicate waste [8-11], a wide range of materials as expanding agents [5, 12-15] and additives [13, 16-18] as well as other ways of more efficient heat treatment of raw material mixture [19]. The purpose of this research is to obtain improved physical, thermal, and mechanical characteristics of glass foams, the use in the process of some natural products or industrial by-products considered wastes and increasing the energy efficiency of the manufacturing process by using unconventional techniques.

The current work is focused on glass foam manufacturing processes using a liquid expanding agent. The advantage of this type of agent compared to the preominantly used solid agents is the possibility of its easy spread through the free spaces between the fine particles of raw material mixture providing excellent conditions for homogeneous contact between the two phases. Consequently, a fine and evenly distributed microstructure of the foam is relatively easy to obtain folowing the sintering/foaming process.

The use in industrial production of glass foam gravel of glycerine as a liquid carbonaceous foaming agent is known from the literature. The peculiarity of this proces is the association of glycerine with sodium silicate (also called water glass) as an enveloping material for the fine carbon particles resulted by the thermal decomposition of glycerine preventing its premature oxidation [20, 21].

Industrially, the German company Glapor Werk Mitterteich uses a manufacturing recipe composed of recycled glass waste (87 %), glycerine (1 %), water glass (12 %), and minor quantities of kaolin (less than 0.5 %) [22]. According to the company's technical report [23], the main characteristics of the cellular product are: bulk density (compressed fill) between 0.125-0.155 g cm^{-3}, heat conductivity (compressed fill) of 0.078 W $(mK)^{-1}$, compressive strength (10 % compression) above 0.6 MPa. The advantages of the porous material manufactured by Glapor with liquid foaming agent are: light weight, the density of glass foam being only 20 % of the density of ordinary aggregates, excellent thermal insulating properties due to porosity with many cosed cells, resistance to acids, bases, bacteria, frost, moisture, fire, rodents and insects, water permeability. The material has applications in the following fields: load-bearing thermal insulation for foundation slabs with perimeter insulation, insulation under the ceiling, terraces, and balconies, flat roof insulation, road insulation, etc.

Recent research has aimed to test the use of water glass as the sole liquid foaming agent of glass waste without another common agent. The main reason was the high price of glycerine around 2800 USD/ton both in European markets and in the United States [24] compared to the price of a solid foaming agent widely used in glass foam manufacturing processes (calcium carbonate) which on European markets reaches 297 USD/ton.

The paper [25] presents experimental results obtained in the manufacture of glass foam from colored container glass waste with a grain size of 75, 150 and 250 μm as raw material and sodium silicate (water glass) as an expanding agent (in proportion of 15 %). The starting mixture was uniaxially pressed at 10 MPa and sintered successively at 800 and 850 ºC in a conventional oven. The results showed that the lowest grain size of the glass waste (75 μm) and the sintering temperature of 800 ºC were the optimal parameters for obtaining specimens with homogeneous microstructure characterized by small and closed pores. Glass grain size and higher temperatures led to coarse microstructures that negatively influenced the mechanical strength and heat conductivity of the specimens.

The thermal process of foaming glass waste using only water glass as an expanding agent was also experimented and presented in the paper [26]. Glass foam with very fine porosity and closed cells with a diameter of less than 0.8 mm was manufactured by the method of conventional heating of the pressed mixture of glass powder and aqueous solution of water glass. The optimum temperature of the heat treatment was between 800-850 ºC. The weight ratio of water glass tested in this experiment varied between 6-24 %, the thermal conductivity of the glass foam having decreasing values from 0.30 to 0.15 W $(mK)^{-1}$. The minimum value of thermal conductivity was achieved after the sintering process at 800 ºC. The compressive strength of 1.7 MPa could be achieved. The microscopic configuration of glass foam specimens showed the homogeneous distribution of closed cells that favors the thermal insulating properties of the material.

Another paper [27] includes in its content the possibility of using the aqueous solution of sodium silicate as the only foaming agent in the process of making glass foam. Analyzing the role of the addition of water glass in the mixture of cathode ray tube (CRT) panel glass, Mn_3O_4 and carbon as a foaming agent, the paper also investigates the peculiarities of using only sodium silicate mixed with CRT panel glass waste. The aqueous solution of water glass releases water during the heating process of the mixture, observed at temperatures above 400 ºC. Practically, by heating the water glass begins to foam by itself. However, the stability of the glass foam thus obtained is poor. Experimentally, it has been shown that water glass can be used as the sole foaming agent for the production of glass foam without the contribution of another ordinary agent. However, the heat conductivity of the foam has quite high values. In the experiment presented in [27], the weight proportion of water glass was between 0-24 %. It is assumed that the contribution of water glass as a foaming agent is based on the release of more strongly bound water. Often before the heating process begins for sintering, the solid material mixture is dried. Thus, the water content decreases with the release of water with less strong bonds. The glass foam produced from dry mixture has lower density and smaller pore size compared to the foam obtained from a wet mixture when heated to the same temperature. According to the results, the specimens of glass foam prepared at a lower foaming temperature from mixtures containing 24 % water glass had a density similar to that of specimens from mixtures with 12 % water glass at higher foaming temperature. In both cases the increase of the foaming temperature over 800 ºC led to the increase of the proportion of open porosity simultaneously with the increase of the pore size. The heat conductivity of glass foam containing 12 % water glass varied between 0.040-0.063 W $(mK)^{-1}$ and that of the foam containing 24 % water glass had values between 0.043-0.050 W $(mK)^{-1}$.

The research that was the basis of the current paper aimed to test the manufacture of glass foam from colorless post-consumer drinking bottle using only aqueous solution of sodium silicate as a foaming agent. The originality of the experiment was the application of the unconventional microwave heating technique, unlike the conventional methods used in the experiments presented above.

2. Methods and materials

Aqueous solutions of soluble sodium silicates in which the SiO_2/Na_2O ratio is higher than 1.5 are known as water glass. The sodium silicate water glass has an adhesive nature and this property is more accentuated with the reduction of the water content. These materials dehydrate easily. Sodium silicate solutions, especially those with a higher SiO_2/Na_2O ratio, are used as an adhesive. Research on the $Na_2SiO_3 \cdot xH_2O$ system has shown the existence of five crystalline sodium metasilicates that are hydrates containing 5-9 molecules of water in addition to the anhydrous material [28]. According to [29], the contact between a soda-lime glass and a neutral or slightly alkaline aqueous solution causes an exchange of hydrogen-alkali ions by a controlled diffusion. The silica network remains stable and is not affected. The method of foaming glass waste using water glass is based on breaking water crystallization bonds and releasing it in the form of vapor. The released water vapors are blocked in the thermally softened mass of the glass forming bubbles, which by cooling turn into a network of pores specific of glass foam.

Unlike the experiments described in [25-27], performed by conventional heating methods, the tests on foaming glass waste using aqueous solution of water glass presented in this paper were performed by applying the own predominantly direct microwave heating technique [19]. 800 W-microwave oven of the type usually used in the household but constructively adapted for high temperatures (above 1000 ºC) was the experimental equipment. The raw material mixed with the aqueous solution of water glass and pressed was freely deposited on a metal support placed on the ceramic fiber thermal insulation at the base of the oven. A cylindrical ceramic tube of SiC and Si_3N_4 with the diameter of 125 mm, height of 100 mm and wall thickness of 2.5 mm was placed between the pressed material and the emission source of the microwave field. The tube had a lid made of the same material. Because the peculiarity of the direct microwave heating consists in initiating the process in the core of material [30, 31] inverse to the conventional heating, efficient thermal protection with ceramic fiber mattresses of the outer surface of the ceramic tube and lid was required. A radiation pyrometer axially mounted above the oven visualizing the heated material through 30 mm-holes provided in the upper wall of the oven and the ceramic lid allowed the control of its temperature evolution. The experimental microwave equipment is shown in Fig. 1.

a b c

Fig. 1. Experimental microwave equipment
a – 800 W-microwave oven; b – thermal protection of ceramic tube and lid; c – ceramic tube.

The raw material used in experiment was recycled glass waste coming from colorless post-consumer drinking bottle. The oxide composition of this glass type contains: 71.7 % SiO_2, 1.9 % Al_2O_3, 12.0 % CaO, 1.0 % MgO, 13.3 % Na_2O, and 0.1 % other oxides. Waste processing included the following operations: selection by color, washing, drying, breaking, grinding in a ball mill, and sieving. The grain size of glass after these operations was below 60 μm. The water glass was purchased from the market as a 30 % aqueous solution.

The characterization of the glass foam specimens was performed by the following methods. The gravimetric method [32] was used to determine the apparent density and the method of comparing the "true" density with the apparent density [33] was used to calculate the porosity of the specimens. Determining the heat conductivity was performed by the heat-flow method (ISO 9869-1: 2014, reviewed and confirmed in 2019) and the TA.XTplus Texture analyzer was used to identify the compressive strength (EN 826-2013). To measure the volumetric proportion of absorbed water in the material it was applied the method of specimen immersion in water (for 24 hours) (ASTM D570). The microstructural peculiarities of cellular glass-ceramic specimens were examined with ASONA 100X Zoom Smartphone Digital Microscope.

3. Results and discussion

Three experimental variants were adopted for the mixture including glass waste, water glass, and distilled water as an additional binder. The weight proportions of these components are presented in Table 1. The ranges of component dosage values were chosen based on the results of previous preliminary tests.

Table 1

Composition of the experimental variants

Variant	Glass waste (wt. %)	Water glass (wt. %)	Distilled water (wt. %)
1	83.0	12.0	5.0
2	81.5	12.5	6.0
3	80.0	13.0	7.0

Mixing the fine glass waste powder with water glass and distilled water in the proportions indicated in Table 1 led to obtaining a sludge, which was loaded into a cylindrical metal mold with a detachable wall in which it was axially pressed at approx. 2-3 MPa. The compacted wet mass was then removed from the mold and freely placed in the microwave oven. In all experimental variants the amount of wet material was kept constant at 480 g.

The heating process for the manufacture of glass foam carried out in the microwave oven had the functional parameters shown in Table 2.

Table 2

Functional parameters of the process

Variant	Wet raw material/glass foam amount (g)	Sintering/ expanding temperature (ºC)	Heating time (min)	Average rate (ºC/min)		Index of volume increasing	Specific energy consumption (kWh/kg)
				Heating	Cooling		
1	480/385.5	788	28	27.4	6.0	1.35	0.76
2	480/385.1	793	28.5	27.1	5.8	1.45	0.77
3	480/384.6	808	30	26.3	5.8	1.90	0.81

According to the data in Table 2, the measured temperature of the end of sintering and foaming process of raw material was in the range 788-808 ºC, the highest value corresponding to the maximum addition of water glass and distilled water (variant 3). Due to the remarkable energy efficiency of the predominantly direct microwave heating, the average heating rate reached very high values (26.3-27.4 ºC/min) and the process time was short (between 28-30 min). Implicitly, the specific energy consumption was in a very small range of values (0.76-0.81 kWh/kg).

The appearance of the glass foam specimens in cross section obtained following the experimental manufacturing process is shown in Fig. 2. The images indicate the fineness of the microstructure of specimens 1 and 2 sintered at temperatures below 800 ºC and having in the starting mixture lower proportions of water glass and distilled water. The specimen 3 sintered at 808 ºC and having the highest proportions of water glass and water is characterized by a less fine, but homogeneous microstructure with closed pores whose size does not exceed 1 mm.

a b c

Fig. 1. Appearance of glass foam specimens
a – specimen 1 heated at 788 ºC; b – specimen 2 heated at 793 ºC;
c – specimen 3 heated at 808 ºC.

The investigation of the physical, thermal, mechanical, and microstructural characteristics of the glass foam specimens performed with the methods indicated above allowed identifying the peculiarities of each specimen. Table 3 shows the results of these investigations.

Table 3

Physical, thermal, mechanical, and microstructural features of specimens

Variant	Apparent density (g cm^{-3})	Porosity (%)	Heat conductivity [W $(mK)^{-1}$]	Compressive strength (MPa)	Water absorption (vol. %)	Pore size (mm)
1	0.33	84.3	0.069	1.85	1.5	0.10 – 0.30
2	0.30	85.7	0.065	1.73	1.1	0.20 – 0.50
3	0.25	88.1	0.059	1.40	0.9	0.40 – 0.90

Analyzing the data from Table 3, the thermal insulating properties of the experimentally obtained foams can be noticed being determined by the low values of the apparent density (0.25-0.33 g cm^{-3}) and of the heat conductivity [0.059-0.069 W $(mK)^{-1}$] as well as the high values of porosity (84.3-88.1 %). The compressive strength is within the acceptable limits of glass foams usable as thermal insulation material (1.40-1.85 MPa). Also, the porous material is not water absorbent, the volumetric proportion experimentally determined being only between 0.9-1.5 vol. %.

Examining the microstructural configuration of the glass foam specimens (Fig. 3) confirms the fineness of their microstructure and homogeneity of the pore distribution in the material section. The pore size of maximum 0.90 mm is indicated in Table 3.

Fig. 3. Microstructural configuration of glass foam specimens
a – specimen 1; b – specimen 2; c – specimen 3.

The experiment described in the paper confirmed that the use of aqueous solution of sodium silicate as the only glass expanding agent is feasible and does not require a commonly more expensive agent for similar processes of manufacturing a glass foam with thermal insulation properties required in the building. The main difference between adopting the unconventional technique of predominantly direct microwave heating compared to the conventional methods applied in the experiments [25-27] mentioned above is the very high heating rate (26.3-27.4 ºC/min) compared to much lower values (under 15 ºC/min) recommended in the literature [1] without affecting the homogeneous organization of the microstructure of final products. The consequence of this advantage is the high level of energy efficiency of the unconventional technique, the specific energy consumption being diminished up to 0.76 kWh/kg. Glass foam manufacturers do not provide clear information on the energy efficiency of their conventional manufacturing processes. However, it can be deduced that even in continuous industrial conditions a value below this limit cannot

be obtained. Moreover, according to [34] the transition from a small-scale experiment to an unconventional industrial-scale process could increase its energy efficiency by up to 25 %.

4. Conclusions

The paper aimed to test the use of aqueous solution of sodium silicate as the only foaming agent in the experimental manufacturing process of glass foam from recycled glass waste without the contribution of another commonly used agent. The originality of the process was the application of the own technique of predominantly direct microwave heating unlike conventional methods of heat treatment of the powder mixture composed of glass and foaming agent. The predominantly direct microwave heating controlled by the wall thickness (2.5 mm) of a ceramic screen made of strongly microwave susceptible materials placed between the source emitting electromagnetic waves and the irradiated material allowed to reach very high heating rates (between 26.3-27.4 ºC/min) compared to their recommended range (5-15 ºC/min) used in industrial processes. Glass foam produced by sintering at 788-808 ºC had thermal insulation properties suitable for building materials (density between 0.25-0.33 g cm^{-3}, heat conductivity between 0.059-0.069 W $(mK)^{-1}$, porosity between 84.3-88.1 %) as well as compressive strength between 1.40-1.85 MPa. The excellent energy efficiency of the heating technique led to very economical specific energy consumptions (between 0.76-0.81 kWh/kg).

References

[1] G. Scarinci, Giovanna Brusatin, E. Bernardo, „Glass Foams" in Cellular Ceramics: Structure, Manufacturing, Properties and Applications, Wiley-VCH Verlag GmbH & Co KGaA, M. Scheffler, P. Colombo eds., Weinheim, Germany, 2005, pp. 158-176.

[2] *** „Glass recycling-Current market trends", Recovery, no. 5, 2018. https://www.recovery-worldwide.com/en/artikel/glass-recovery-current-market-trends_3248774.html

[3] L. Paunescu, S.M. Axinte, M.F. Dragoescu, Felicia Cosmulescu, „Adequate correlation between the physical and mechanical properties of glass foam", Journal La Multiapp, vol. 2, no. 4, 2021, pp. 14-26.

[4] H.W. Guo, Y.X. Gong, S.Y. Gao, „Preparation of high strength foam glass-ceramics from waste cathode ray tube", Materials Letters, vol. 64, no. 8, 2010, pp. 997-999.

[5] R.R. Petersen, J. Kőnig, M.M. Smedskjaer, Y. Yue, „Foaming of CRT panel glass powder using Na_2CO_3", Glass Technology, vol. 55, no. 1, 2014. https://www.researchgate.net/publication/263524095_Foaming_of_CRT_panel_glass_powder_using_Na_2CO_3

[6] Rosa Taurino, Isabella Lancellotti, Luisa Barbieri, Cristina Leonelli, „Glass-ceramic foams from borosilicate glass waste", International Journal of Applied Glass Science, 2014, pp. 1-10. https://doi.org/10.1111/ijag.12069

[7] A.V. Gorokhovsky, J.I. Escalante Garcia, J. Mendez-Nonell, V.A. Gorokhovsky, D.V. Mescheryakov, „Foamed glass-ceramic materials based on oil shale by-products", Glass Science and Technology, vol. 75, no. 5, 2002, pp. 259-262.

[8] M. Zhu, R. Ji, Z. Li, Z. Zhang, „Preparation of glass ceramic foams for thermal insulation applications from coal fly ash and waste glass", Construction and Building Materials, vol. 112, no. 1, 2016, pp. 398 – 405. https://www.researchgate.net

[9] Emilija Fidancevska, B. Mangutova, M. Milosevski, D. Milosevski, J. Bassert, „Obtaining of dense and highly porous materials from metallurgical slag", Science of Sintering, vol. 35, no. 2, 2003, pp. 85-91.

[10] Z. Li, Z. Luo, X. Li, T. Liu, L. Guan, T. Wu, A. Lu, „Preparation and characterization of glass ceramic foams with waste quartz sand and coal gangue in different proportions", Journal of Porous Materials, vol. 23, 2016, pp. 231-238.

[11] M. Pelino, „Recycling of zinc-hydrometallurgy wastes in glass and glass ceramic materials", Waste Management, vol. 20, no. 7, 2000, pp. 561-568.

[12] Sabrina Arcaro, Bianca Goulart de Oliveira, M. Tramontin Souza, F.R. Cesconeto, Laura Granados, A.P. Novaes de Oliveira, „Thermal insulating foams produced from glass waste and banana leaves", Material Research, vol. 19, no. 5, 2016, pp. 1064-1069. http://dx.doi.org/10.1590-1980-5373-MR-2015-0539

[13] A.S. Llaudis, M.J. Orts Tari, F.J. Garcia Ten, E. Bernardo, P. Colombo, „Foaming of flat glass cullet using Si_3N_4 and MnO_2 powders", Ceramics International, vol. 35, no. 5, 2009, pp. 1953-1959.

[14] Y. Attila, M. Güden, A. Tasdemirci, „Foam glass processing using a polishing glass powder residue", Ceramics International, vol. 39, 2013, pp. 5869-5877.

[15] H.R. Fernandes, Diana D. Ferreira, Fernanda Andreola, Isabella Lancellotti, Luisa Barberi, J.M.F. Ferreira, „Environmental friendly management of CRT glass by foaming with waste egg shells, calcite or dolomite", Ceramics International, vol. 40, no. 8, 2014, pp. 13371-13379.

[16] Sara Abbasi, S.M. Mirkazemi, A. Ziaee, Mina Saeedi, „The effect of Fe_2O_3 and Co_3O_4 on microstructure and properties of foam glass soda lime waste glasses", Glass Physics and Chemistry, vol. 40, no. 2, 2014, pp. 173-179.

[17] Q. Zhang, F. He, H. Shu, Y. Qiao, S. Mei, M. Jin, J. Xie, „Preparation of high strength glass ceramic foams from waste cathode ray tube and germanium tailings", Construction and Building Materials, vol. 111, 2016, pp. 105-110.

[18] E. Ercenk, „The effect of clay on foaming and mechanical properties of glass from insulating material", Journal of Thermal Analysis and Calorimetry, vol. 127, no. 1, 2017, pp. 137-146.

[19] S.M. Axinte, L. Paunescu, M.F. Dragoescu, Ana C. Sebe, „Manufacture of glass foam by predominantly direct microwave heating of recycled glass waste", Transactions on Networks and Communications, vol. 7, no. 4, 2019, pp. 37-45. https://doi.org/10.14738/tnc.74.7214

[20] Svitlana N. Karandashova, B.M. Goltsman, E.A. Yatsenko, „Analysis of influence of foaming mixture components on structure and properties of foam glass", IOP Conf. Series: Materials Science and Engineering, vol. 262, 2017. https://iopscience.iop.org>article>262

[21] E.A. Yatsenko, B.M. Goltsman, V.A. Smoliy, A.S. Kosarev, „Investigation of a porous structure formation mechanism of a foamed slag glass based on the glycerol foaming mixture", Research Journal of Pharmaceutical, Biological and Chemical Sciences, vol. 7, no. 5, 2016, pp. 1073-1081.

[22] *** „Environmental Product Declaration", Glapor Werk Mitterteich GmbH, Germany, 2017. https://www.Glapor_cellular_glass_gravel

[23] *** „Glapor cellular glass gravel-Technical data", 2017. https://www.lime.org.uk/fileuploader/download/download/?d=1&file=custom%2Fupload%2FFile-1498740985.pdf

[24] *** „Glycerine price trend and forecast", March 2022. https://www.chemanalyst.com/Pricing-data/glycerine-1168

[25]S.S. Owoeye, G.O. Matthew, F.O. Ovienmhanda, S.O. Tunmilayo, „Preparation and characterization of foam glass from waste container glasses and water glass for application in thermal insulations", Ceramic International, 2020. https://doi.org/10.1016/j.ceramint.2020.01.211

[26] Daniela Hesky, C.G. Aneziris, U. Gross, Anja Horn, „Water and waterglass mixtures for foam glass production", Ceramics International, vol. 41, no. 10, Part A, 2015, pp. 12604-12613. https://doi.org/10.1016/j.ceramint.2015.06.088
[27] U. Hribar, M. Spreitzer, J. Kőnig, „Applicability of water glass for the transfer the glass-foaming process from controlled to air atmosphere", Journal of Cleaner Production, vol. 282, 2021. https://doi.org/10.1016/j.clepro.2020.125428
[28] N.A. MacGilp, „An investigation of some properties of sodium silicates and their use in zeolite synthesis", PhD thesis presented at University of Edinburgh, Scotland, UK, May 1976.
[29] T.M. El-Shamy, C.G. Pantano, „Decomposition of silicate glasses in alkaline solutions", Nature, vol. 266, 1977, pp. 704-706.
[30] D.A. Jones, T.P. Lelyveld, S.D. Mavrofidis, S.W. Kingman, N.J. Miles, „Microwave heating applications in environmental engineering-A review", Resources, Conservation and Recycling, vol. 34, no. 2, 2002, pp. 75-90.
[31] Helen J. Kitchen, S.R. Vallance, Jennifer L. Kennedy, Nuria Tapia-Ruiz, Lucia Carassiti, A. Harrison, „Modern microwave methods in solid-state inorganic materials chemistry: From fundamentals to manufacturing", Chemical Reviews, vol. 114, no. 2, 2014, pp. 1170-1206.
[32] *** „Metrology in laboratory-Measurement of mass and derived values", Radwag Balances and Scales, 2nd edition, Radom, Poland, 2015, pp. 72-73. http://www.radwag.com
[33] L.M. Anovitz, D.R. Cole, „Characterization and analysis of porosity and pore structures", Reviews in Mineralogy and Geochemistry, vol. 80, 2005, pp. 61-164.
[34] Oxana V. Kharissova, B.I. Kharissov, J.J. Ruiz Valdés, „Review: The use of microwave irradiation in the processing of glasses and their composites", Industrial & Engineering Chemistry Research, vol. 49, no. 4, 2010, pp. 1457-1466.